Summary for Policymakers

Drafting Authors:
Paola A. Arias (Colombia), Kyle Armour (USA), Nicolas Bellouin (UK, France), Christophe Cassou (France), Sarah Connors (France, UK), Erika Coppola (Italy), Aida Diongue Niang (Senegal), Alessandro Dosio (Italy), Hervé Douville (France), Piers Forster (UK), Baylor Fox-Kemper (USA), Jan Fuglestvedt (Norway), John Fyfe (Canada), Nathan Gillett (Canada), Ed Hawkins (UK), Richard Jones (UK), Darrell Kaufman (USA), Jim Kossin (USA), Gerhard Krinner (France), June-Yi Lee (Republic of Korea), Jochem Marotzke (Germany), Valérie Masson-Delmotte (France), Vaishali Naik (USA), Friederike Otto (UK, Germany), Matthew Palmer (UK), Anna Pirani (Italy, UK), Gian-Kasper Plattner (Switzerland), Krishnan Raghavan (India), Joeri Rogelj (Austria, Belgium), Maisa Rojas (Chile), Alexander Ruane (USA), Bjorn H. Samset (Norway), Pedro Scheel Monteiro (South Africa), Sonia I. Seneviratne (Switzerland), Jana Sillmann (Norway, Germany), Anna Amelia Sörensson (Argentina), Sophie Szopa (France), Claudia Tebaldi (USA), Peter Thorne (Ireland, UK), Bart van den Hurk (Netherlands), Robert Vautard (France), Panmao Zhai (China), Xuebin Zhang (Canada), Kirsten Zickfeld (Canada, Germany)

Contributing Drafting Authors:
Katherine Calvin (USA), Pep Canadell (Australia), Mathias Hauser (Switzerland), Sergey Gulev (Russian Federation), Chao Li (China), Brian O'Neill (USA), Roshanka Ranasinghe (Netherlands, Sri Lanka, Australia), Keywan Riahi (Austria), Clemens Schwingshackl (Italy, Norway), Trude Storelvmo (Norway), Emilie Vanvyve (Belgium, UK), Carolina Vera (Argentina), Sönke Zaehle (Germany)

Date of Draft:
03/03/2020

Notes:
TSU compiled version

Introduction

The Working Group I (WGI) contribution to the IPCC's Sixth Assessment Report (AR6) provides an updated state of knowledge related to the climate system and climate change, based on the assessment of evidence available in the scientific literature related to the climate system (the atmosphere, ocean, land surface, cryosphere and biosphere). This report builds upon the WGI contribution to the IPCC's Fifth Assessment Report (AR5), and the three Special Reports in the sixth assessment cycle (SR1.5, SROCC and SRCCL).

This Summary for Policymakers (SPM) is structured in four parts, A: Understanding human-induced climate change and communicating climate information, B: The current state of the climate: where are we now and how did we get here? C: Our possible climate futures and D: Climate information to support mitigation and adaptation action. Each part is supported by a series of overarching highlighted conclusions which, taken together, provide a concise summary. Main sections are introduced with a brief paragraph in italics which outlines the methodological basis of the assessment.

Confidence in key findings is indicated using the IPCC calibrated language[1]. Probabilistic estimates of quantified measures of uncertainty in a finding are based on statistical analysis of observations or model results, or both, and expert judgment[2]. Where appropriate, findings are also formulated as statements of fact without using uncertainty qualifiers. Variations in observed and simulated climate variables are often presented as differences relative to the average value over a multi-decadal 'baseline' or 'reference period'[3].

[START BOX SPM.1 HERE]

Box SPM.1: Core concepts central to this report

This box provides a discussion of key concepts and definitions which are relevant to the AR6 assessment, with a focus on those which have been updated or are new since AR5.

Global surface temperature indicators: Global surface air temperature (GSAT) is used as the principal surface temperature metric throughout this report. This is a distinct choice compared to AR5 and the three AR6 cycle special reports. An adjustment is applied to observed global mean surface temperature (GMST) products to account for non-equivalence between GSAT and GMST that is growing as the climate system

---

[1]Confidence is a qualitative measure of the validity of a finding, and is expressed using five qualifiers: very low, low, medium, high, and very high, and, where possible, probabilistically with a quantified likelihood. Assessed confidence is typeset in italics, e.g., *medium confidence*. Likelihood provides a quantified measure of uncertainty in a finding expressed probabilistically and the following terms are used: *virtually certain* (99–100% probability), *extremely likely* (95–100%), *very likely* (90–100%), *likely* (66–100%), *more likely than not (*50–100%), *about as likely as not* (33–66%), *unlikely* (0–33%), *very unlikely* (0–10%), *extremely unlikely* (0–5%), *exceptionally unlikely* (0–1%). This Report also uses the term '*likely* range' or '*very likely* range' to indicate that the assessed likelihood of an outcome lies within the 17–83% or 5–95% probability range. Assessed likelihood is typeset in italics, e.g., *very likely.*

[2]Throughout this WGI report and unless stated otherwise, uncertainty is quantified using 90% uncertainty intervals. The 90% uncertainty interval, reported in square brackets [x to y], is expected to have a 90% likelihood of covering the value that is being estimated.

[3]Paleoclimate reference periods predate the pre-industrial period and provide additional context for understanding causes of variations in Earth's climate. 1750 is understood as 'pre-industrial', though the period 1850-1900, when permanent surface observing networks that provide sufficiently accurate and continuous measurements on a near-global scale started, is used as a pragmatic approximation for pre-industrial global temperature. The 'modern period' is defined as 1995–2014. The historical period in CMIP6 simulations ends in 2014. In AR5 the equivalent period was 1986-2005 for the same reason. Three future reference periods are defined: 'near-term' (2021–2040), 'mid-term' (2041–2060) and 'long-term' (2081–2100). {Cross Chapter Box 1.2, Cross Chapter Box 2.1, 1.4.1}

continues to warm[4]. {Cross Chapter Box 2.3}

Global warming levels: This report frequently uses the concept of specific warming levels such as 1.5°C, 2°C or 3°C – defined as changes in GSAT relative to either the pre-industrial (year 1750) or the 1850–1900 reference periods – to assess and communicate information about global and regional changes, impacts, and emissions and concentration scenarios. {1.6.2, 11.1, 11.2, 12.5.2, Cross-Chapter Box 1.5, Glossary}

Climatic impact drivers: The term 'climatic impact drivers' is used to describe natural or human-induced climate-related physical events or trends that may have detrimental (hazards) or beneficial impacts on elements of society or ecosystems. {12.1, Cross Chapter Box 1.3, Glossary}.

Risk framework: A common framework for describing and assessing risk across all three working groups is adopted to promote clear and consistent communication of risks and to better inform risk assessment and decision making related to climate change. {Cross Chapter Box 1.3, Glossary}

Storylines: The storylines approach can be used to explore uncertainties in climate change, to develop integrated and context relevant messages of regional changes, and to address issues with deep uncertainty, including low-likelihood, high-impact events. {1.4, 4.8, Box 9.3, 10.5.3, 11.2.4, Atlas.6.1.5, Glossary}

Low-likelihood, high impact events: These are events whose probability is low but whose potential impacts on society and ecosystems are high. To better inform risk assessment and decision making, such low-likelihood outcomes are described as they may be associated with very high levels of risk and because the greatest risks might not be associated with the most likely outcome. { 4.8, 7.5, 11.2, 11.3, 11.4, Cross Chapter Box 1.3}

Internal and natural variability: Internal variability refers to climatic fluctuations that occur naturally in the absence of any change in radiative forcing, for example the El Nino Southern Oscillation. Natural variability refers to climatic fluctuations that occur without any human influence, i.e. internal variability combined with the response to external natural factors such as volcanic eruptions and changes in solar activity. {1.4, 1.5, 2.2, 2.4, 3.3, 3.5, 3.7, 4.4, 4.5, 4.6, 7.2, 8.2, 8.5, 9.2, 10.3, 10.4, 11.7, Box 4.1, Glossary}

Emergence: When a change in climate (the 'signal') becomes larger than the amplitude of natural or internal variations (defining the 'noise'), it is termed to have 'emerged'. This concept is often expressed as a 'signal-to-noise' ratio and emergence occurs at a defined threshold of this ratio. Emergence can refer to changes relative to a historical or modern baseline, and can be expressed in terms of time or in terms of a global warming level. Emergence can be estimated using observations and/or model simulations. {1.4.2, 7.5.5, 10.3, 10.4, Glossary}

[END BOX SPM.1 HERE]

[4]There is *high confidence* that GMST and GSAT differ and an adjustment of 4% (2-7%) is required to be applied to GMST estimates and their range to infer GSAT equivalent estimates {Cross-Chapter Box 2.3}.

A. Understanding the emergence of human-induced climate change and communicating information

PREAMBLE: *This SPM summarises our current understanding of climate science, based on multiple lines of evidence, including many independent scientific analyses from observations of the climate system; paleoclimate archives; theory and understanding of physical, chemical and biological processes; and simulations using climate models. This introduction focuses on the evidence base and how that evidence allows new assessments about changes in regional climate. It also discusses the core concepts and definitions used throughout AR6 WGI, with a particular focus on risk, and plausible events that would have a high impact but are uncertain in their chance of occurrence. A significant innovation in the AR6 WGI report is the Atlas which includes an online interactive tool with flexible spatial and temporal analyses of observed and projected climate change information.*

A.1 Evidence base about how and why the Earth's climate varies naturally, and is responding to human perturbations

Several centuries of climate science research have increased knowledge about how Earth's climate varies naturally and how it responds to human perturbations. These advances are the result of more and higher quality observations, expanded information about past climates, improvements in theoretical understanding, and the development of more comprehensive climate models. Due to these multiple independent lines of evidence, human influence on the climate system since the mid-20th century is now an established fact. (Figure SPM.1, Figure SPM.2) {1.2, 1.3, 1.5, 2.3, 3.3, 3.4, 3.5, 3.6, 3,7, 3.8, 10.3, Cross- Chapter Box 2.1, Chapter Box 7.2, Chapter Box 9.2}

A.1.1 Knowledge of key features of the climate system is robust and well established, with the circulation of the atmosphere and ocean having been studied since the 17th-century. The roles of water vapour, carbon dioxide and methane as major heat-absorbing gases were identified in the 19th-century, the principal drivers of natural climate variability (orbital changes, the solar cycle and volcanic activity) have been studied since the early 20th-century, and other major human-related drivers, such as aerosols and land-use change, were described by the mid-1970s. {1.3.3, 1.3.4}

A.1.2 Observations provide unequivocal evidence of a changing climate: the atmosphere and ocean have warmed, ice and glacier mass has diminished, sea levels have risen, patterns of precipitation and extreme weather have changed, ocean pH has declined, and greenhouse gas concentrations in the atmosphere have increased. Evidence of the biosphere's response to a warming climate is consistent with these observed physical indicators. Many climate components are now in states not experienced for centuries to millennia or longer, and since 1900 several key indicators of the global climate system have changed at a rate unprecedented over at least the last two thousand years. (Figure SPM.1, Figure SPM.2) {1.2.1, 2.3.1, 2.3.5}

A.1.3 Since AR5 and SROCC, multiple lines of evidence have built confidence in new related observations of two fundamental aspects of Earth's climate system: the rate of change of global sea level and Earth's energy budget. Observations of each of the major contributors to global sea level rise (melting glaciers and ice sheets in Antarctica and Greenland, ocean warming, changing storage of water on land) *very likely* agree with the observed global sea level rise over the period 1971-2018. The observed increases in Earth's energy (more than 90% of which is ocean warming) are *very likely* consistent with revised estimates of effective radiative forcing and Earth's radiative response. {Chapter Box 7.2, Cross-Chapter Box 9.2}

A.1.4 The accuracy of early climate change projections published since the 1980s can now be assessed against up to 40 years of observations. The pattern of temperature change is in close agreement with what has since been observed, as well as the rate of warming, especially when accounting for differences between the emission scenarios they used and the actual emissions that occurred. {1.3.6}

A.1.5 The latest generation of climate models[5] has a more comprehensive representation of physical and biogeochemical processes relative to previous generations. For most large-scale indicators of climate change, the ability to simulate the observed mean climate and some aspects of the variability has improved compared to the models assessed in the AR5 (*high confidence*). Global high-resolution models exhibit reduced biases in some but not all aspects of surface and ocean climate (*medium confidence*). Regional climate models add value in representing many regional weather and climate phenomena, in particular over complex terrain, and simulations at kilometre-scale resolution add value to the representation of convection *(high confidence*) and many local-scale phenomena such as the diurnal cycle, land-sea breezes and precipitation extremes (*medium confidence*). {1.5.3, 1.5.4, 2.3.1, 3.3.1, 3.3.3, 3.7.3, 3.8.2, 8.5.1, 10.3.3, 10.3.4, Cross-Chapter box 1.2, Cross-Chapter box 2.3}

A.1.6 The IPCC Second Assessment Report (1995) identified a discernible human influence on the climate. Since then and throughout subsequent assessments (TAR, 2001; AR4, 2007; SREX, 2012; and AR5, 2013), the evidence for human influence on the climate system has progressively strengthened. AR5 concluded that human influence on the climate system is clear, evident from increasing greenhouse gas concentrations in the atmosphere, positive radiative forcing, observed warming, and physical understanding of the evolving climate system. This evidence is now even stronger and it is now an established fact in AR6 that human activity has altered the climate system since the mid-20th century. {3.3, 3.4, 3.5, 3.6, 3.7, 3.8}

[START FIGURE SPM.1 HERE]

Figure SPM.1: The intent of this figure is to highlight that multiple climate indicators show that changes are emerging across the climate system, from the atmosphere to the ocean to the cryosphere and biosphere. This emergence is seen over the instrumental record (1850-2018) and over the last 2000 years. Indicators are (from top to bottom): atmospheric carbon dioxide concentration, ocean heat content, global sea level, GMST from HadCRUT5, GMST from PAGES2k, Kyoto cherry blossom date, global lower tropospheric temperature from RSS, Arctic September sea ice extent. Key moments in the history of climate science are indicated: the invention of the efficient steam engine by James Watt in 1790, the identification of the primary greenhouse gases by John Tyndall in 1861, the first estimate of climate sensitivity by Svante Arrhenius in 1896, and the discovery that the world was warming by Guy Callendar in 1938.Quantitatively, the CO_2 concentration increased by 40% over 1850-2018, the ocean heat content increase since 1860 is equal to 430ZJ and the global sea level rose by 18cm since 1900. The GMST increased by 1.1ºC over 1850-2018 while the warming estimated from paleo GMST is equal to 0.65ºC over 1850-2000 and the troposphere warmed by 0.67ºC during the satellite era. Sea ice declined in the Arctic in summer by 35% since 1979.

[END FIGURE SPM.1 HERE]

[START FIGURE SPM.2 HERE]

Figure SPM.2: The intent of this figure is to summarise change across all components of the Earth System including the observed magnitudes over the periods included therein, and to include uncertainty ranges and associated confidences. Options for visualising key indicators of climate includes approaches used FAQ2.2 Figure 1 and also the SROCC Figure TS.2.

[5] Models assessed within the Coupled Model Intercomparison Project Phase 6 (CMIP6)

[END FIGURE SPM.2 HERE]

A.2 From global to regional scales

Human-induced climate trends are superimposed on natural decadal or multi-decadal climate variability, whose effects are more pronounced at regional scales than at the global scale, and relatively larger for most water-cycle variables, including precipitation, than for temperature. The increase in surface temperature over land, especially in the tropics, and the decline in Arctic sea ice are already clearly discernible from natural variations. In terms of future emergence, the relative strength of internal variability and human-induced trends will depend on the region, the variable, and the level of global warming (*high confidence*). {1.4, 3.3, 3.4, 3.5, 4.4, 4.5, 4.6, 8.4, 8.5, 9.3, 9.6, 10.3, 10.4, 11.4, Atlas.6, Cross-Chapter Box 3.1}

A.2.1 Natural variability can temporarily either dampen, mask or enhance multi-decadal human-induced trends with a larger influence at regional scales and for variables related to the water cycle. There is *very high confidence* that temporary periods of both damping and enhancement of underlying human-forced trends will continue to occur on decadal timescales in the 21st century. {1.4.2, 3.3.1, 3.5.1, 8.5.1, 8.5.2, 10.4.1, Cross-Chapter Box 3.1}

A.2.2 Understanding and quantification of the relative roles of internal variability and forced change in the climate system have been improved since AR5, especially at regional scales, based on the more systematic use of large ensembles of simulations covering the historical period and future scenarios. It is *likely* that the role of internal variability has been underestimated in projections in some regions in previous assessments. {10.3.4}

A.2.3 Observed warming in the 1998-2012 period is consistently larger in updated observational products than those assessed in AR5. Subsequent analyses have confirmed that the observed reduced rate of warming relative to earlier decades was due to the combined influence of solar and volcanic forcing and internal variability, with notable regional contributions from the Pacific and from a large part of Eurasia and North America in boreal winters (*high confidence*), in broad agreement with the AR5 assessment. It is *virtually certain* that global ocean heat content continued to increase throughout this period, and the slowdown was only evident in the atmosphere and surface *(very high confidence).* Since 2012, GMST has warmed strongly, with the past five years (2014-2018) being the hottest five-year period in the instrumental record until 2018 (*high confidence*) {3.3.1, 3.5.1, Cross-Chapter Box 3.1}.

A.2.4 Recent increases in annual mean temperature have exceeded levels of year-to-year variations in nearly all continental regions. Tropical land areas exhibit the most clearly discernible emergence, despite the amplitude of warming being smaller than at higher latitudes (*high confidence*). In the Arctic, it is *very likely* that human influence explains more than half of the summer sea ice retreat since satellite measurements began in 1979. {1.4.2, 1.4.3, 9.3.1, 9.3.2, 3.4.1}

A.2.5 Human activities have already affected the water cycle at the global scale (*high confidence*). Model limitations including unresolved small-scale processes hamper strong quantitative model consensus for future hydrological responses at regional scales. Nonetheless, it is *very likely* that internal variability will significantly influence future regional trends in the water cycle over many land regions until at least the mid-21st century. {4.4.1, 4.5.1, 4.6.1, 8.4.1, 8.5.1, 8.5.2, 10.3.4, 10.4.2, 11.4, Atlas.6}

A.2.6 Sea level rise shows distinct regional patterns consistent with the fingerprint of internal decadal variability. Although it is *very likely* that human-caused forcings are the main driver of the observed global mean sea level rise, attribution of past regional changes remain difficult in quantifying consistently all of the contributions to the global sea level before 1971 or all contributions to regional sea level changes. Nonetheless, the human-caused signal in regional sea level change is projected to emerge at over 50% of the ocean area by 2040 regardless of future emissions (*medium confidence*). {3.5.3, 3.4.3, 9.6.1, 9.6.3}

A.3 Integrated Knowledge

Climatic impact drivers that affect natural, managed and human systems are changing with global warming (*high confidence*). Since AR5, there has been considerable progress in understanding user needs, in better facilitation of user engagement and in applying co-design and co-development processes to generate actionable climate information (*high confidence*). The construction and communication of climate change information for risk assessment is strengthened by the use of multiple lines of evidence and the consideration of low-likelihood but potentially high-impact events. (SPM Box.3) {1.1, 1.2, 4.8, 10.3, 10.5, 10.6, 11.2, 12.1, 12.2, 12.3, 12.4, 12.5, Atlas.1, TS.4.1, Box TS5 Figure 3}

A.3.1 A variety of methodologies have been developed to construct impact- and risk-relevant climate change information relevant to a broad range of regional scales. There is *high confidence* that distilling climate messages derived from multiple, potentially contrasting, lines of evidence such as observed, paleoclimate proxy and simulated data, theoretical understanding, diverse analysis methods and expert judgment increases confidence in climate change messages. (SPM Box.3) {10.5.4, 10.6, 12.1, Atlas, TS.4.1, Box TS5 Figure 3}

A.3.2 Climatic impact drivers affecting a wide range of natural and human systems can be measured by tailored indices to represent critical thresholds, multiple variables and their interactions relevant for the specific system. A direct relationship with global warming is identified for many indices describing climatic impact drivers (*medium confidence*). There is *high confidence* that in all regions of the world multiple climatic impact drivers have changed in recent decades, and are projected to continue to change over the 21st century regardless of the emission scenario. (SPM Box.3) {12.2, 12.3, 12.4, 12.5.2}

A.3.3 Communication of scientific understanding and information occurs in the context of implicit and explicit values and beliefs. There is *high confidence* that climate change messages are influenced by the values of those constructing, communicating and receiving the message and there is *high confidence* that by including users, the context for forming the message can be accounted for. {1.2.3, 10.5}

A.3.4 The use of a narrative structure and storylines contributes to building a robust and comprehensive picture of climate information, and related risk. This can explicitly address low-likelihood but potentially high-impact events not reflected in the mean and *likely* range of available model results, especially at regional scales (*high confidence*). Storyline approaches are also a way of exploring, illustrating and communicating uncertainties related to climate change projections. (Box SPM.3) {1.1.4, 4.8, 10.3.4, 10.5.4, 10.6, 11.2.4, Atlas 1.2}

B. The current state of the climate: where are we now and how did we get here?

PREAMBLE: *Our understanding of the current state of the climate system is based on observations extending back to the mid-19th century and proxy indicators of natural climate variability extending back hundreds to millions of years, coupled with climate model simulations and knowledge of climate system processes and feedbacks. This section assesses the natural and anthropogenic drivers that alter the Earth's energy balance, followed by assessment of the current state of the atmosphere, ocean and cryosphere. It concludes with an assessment of extremes, which are particularly relevant to regional hazards and impacts.*

B.1 Earth's energy imbalance

The atmospheric concentrations of carbon dioxide, methane, and nitrous oxide have increased since 1750 to levels unseen in at least 800,000 years (*very high confidence*). It is unequivocal that this increase is due to human activities. Current global carbon dioxide concentrations are unprecedented in at least the last 2 million years (*high confidence*). The perturbation to the Earth's energy imbalance caused by human activity, quantified as effective radiative forcing for 2018 relative to 1750, is 2.53 (1.58 to 3.34) Wm^{-2}, 11% higher than that reported in AR5 for the year 2011. {2.2, 3.1, 5.1, 5.2, 6.2, 7.3, TS2.1}

B.1.1 In 2018, the atmospheric concentration of carbon dioxide (CO_2) was 407 ppm, 15 ppm higher than reported in AR5 (2011) and 129 ppm higher than in 1750. This increase was driven by emissions from human activities, which reached 40.3 (37.3 - 43.3)[6] $GtCO_2$ yr^{-1} on average over 2009-2018. Emissions from fossil fuel combustion and cement production, contributing 81-91% of all anthropogenic CO_2 emissions, grew by 0.9% per year from 2010 to 2018, compared to 3.2% per year in the previous decade. Emissions from land use and land use change, responsible for the remainder of the anthropogenic emissions, were 5.5 (2.9 - 8.1) $GtCO_2$ over 2009-2018. {2.2.3, 5.1.1, 5.2.1, TS2.1}

B.1.2 From 1750 to 2018, fossil fuel combustion and cement production emitted 1613 (1540-1687) $GtCO_2$ while land-use change emitted 862 (587-1137) $GtCO_2$. Of the cumulative total CO_2 emissions, 1008 [990-1027] $GtCO_2$ have accumulated in the atmosphere, 623 (550-696) $GtCO_2$ have been taken up by the ocean and 807 (623-990) $GtCO_2$ have accumulated in land ecosystems. There is *high confidence* that the fraction of excess anthropogenic CO_2 removed by ocean and land has declined, consistent with the expectation that emerging feedbacks will weaken these sinks (*high confidence*). {5.2.1, 5.2.2, 5.2.3}

B.1.3 The atmospheric concentration of methane (CH_4) increased at an average rate of 7.1 ± 2.7 ppb yr^{-1} over 2009–2018 (*high confidence)*, resuming its long-term growth following a period of reduced growth that ended in 2007, and reached 1859 ± 3 ppb in 2018. There is *medium confidence* that the growth in CH_4 since 2007 was largely driven by emissions from fossil fuels and livestock. The atmospheric nitrous oxide (N_2O) concentration increased by 0.80 ± 0.07 ppb yr^{-1} since the 1990s, reaching 331.2 ± 0.3 ppb in 2018 (*high confidence*). Agricultural N_2O emissions have increased by about 30% since the 1980s, with increased use of nitrogen fertiliser and manure contributing about 70% of this increase (*high confidence*). {5.2.3}

[6] 1 Gigatonne of CO_2 = 1$GtCO_2$ = 10^{15} grams of CO_2. This contains 0.273 Gt of carbon (GtC).

B.1.4 Aerosol optical depth[7] has decreased since 2000 over Northern Hemisphere mid-latitudes and Southern Hemisphere mid-latitude continents, but increased over South Asia and East Africa (*high confidence*). Observations show that stratospheric ozone between 60°S - 60°N declined from 1980 to 2018 by 2.2% with most of this decline occurring over 1980-1995 (*high confidence*). Since the mid-1990s, free tropospheric ozone has increased by 2-7 % per decade in northern mid-latitudes, 2-12 % in the tropics (*high confidence*) and <5 % in southern mid-latitudes (*medium confidence*). {2.2.4, 2.2.5, 2.2.6, 6.2.1, TS2.1}

B.1.5 The total effective radiative forcing (ERF) from increases in greenhouse gases from 1750 to 2018 is 3.63 W m^{-2} (3.27 to 3.97 Wm^{-2}), 15% greater than the 2011 estimate in AR5 due to increases in atmospheric concentrations since 2011 and revisions to forcing estimates. CO_2 contributes the largest part of this forcing with a value of 2.15 Wm^{-2} (1.89-2.41 Wm^{-2} range), CH_4 contributes 0.54 W m^{-2} (0.43-0.65 W m^{-2} range), N_2O contributes 0.19 W m^{-2} (0.16-0.22 W m^{-2} range) with synthetic gases, ozone and stratospheric water vapour changes contributing the remainder. There has also been an upward revision in the estimated shortwave forcing from CH_4 since AR5 (*high confidence*). The net ERF attributable to halocarbons is smaller than the direct ERF due to their effect on ozone depletion, such that the range includes zero (0.0 to 0.16 W m^{-2}) *(high confidence*). {7.3.5, TS3.1}

B.1.6 The total ERF from changes in aerosols from 1750 to 2018 is -1.1 (-2.0 to -0.4) W m^{-2}. The ERF due to aerosol–cloud interactions contributes about 3/4 to the magnitude of the total aerosol ERF, with the remainder due to the forcing associated with aerosol-radiation interactions. Compared to the estimates in 2011 for AR5, there has been a doubling of the magnitude of ERF from aerosol cloud interactions, and a downward revision of the magnitude of ERF from aerosol-radiation interactions (*high confidence*). The relative importance of aerosol forcing compared to other forcing agents has decreased at the global scale in the most recent 30 years (*medium confidence*). {2.2.8, 7.3.3, 7.3.5}

B.1.7 Changes in ERF due to solar (-0.01 (-0.05-0.1) Wm^{-2}) and episodic volcanic eruptions since 1750 are small in comparison to other drivers (*high confidence*). Solar activity since 1900 was high but not exceptional compared to the past 9000 years (*high confidence*). The average magnitude and variability of volcanic aerosol forcing since 1900 has not been unusual when compared to the past 2500 years (*medium confidence*). {2.2.1, 2.2.2}

B.2 Atmosphere

Global surface air temperature has increased since 1850, and, over the past fifty years, it has done so at a rate unprecedented in at least the last two thousand years (*medium confidence*). Several aspects of the atmospheric circulation have *likely* changed since the mid-20th century, including widening of the tropical belt and poleward jet migration, and there is *medium confidence* that human influence contributed to these changes. There is *high confidence* that since pre-industrial times human activities have strengthened the global water cycle. (Figure SPM.3, Figure SPM.4, Figure SPM.5) {2.3, 3.3, 3.7, 8.2, 8.3, Box 8.1, Cross-chapter box 1.2}

[7] A measure of the amount of sunlight blocked by aerosols and is related to the amount of aerosol in the vertical column of atmosphere

B.2.1 It is *about as likely as not* that no multi-centennial period since the end of the last interglacial period was warmer globally than the most recent decade. The net increase of global surface air temperature (GSAT) caused by anthropogenic factors between 1750 and 1850-1900 is *likely* -0.1 to 0.2°C (*medium confidence*). From 1850-1900 to 2009-2018, GSAT increased by 1.10°C (0.97° – 1.25°C). The *likely* range of GSAT warming due to increases in well-mixed greenhouse gases from human activities is 0.9°– 2.0°C, and the *likely* range of GSAT change due to aerosols and other anthropogenic forcings is -0.7°– 0.2°C. Temperatures have increased faster over land than over the ocean since 1850-1900, with warming to 2009-2018 of 1.44 °C (1.32 – 1.60 °C) versus 0.89 °C (0.80 – 0.96 °C). (Figure, SPM.3, Figure SPM.4, Figure SPM.5) {2.3.1 Cross-chapter Box 1.2}

B.2.2 The troposphere has warmed since the 1950s, and it is *virtually certain* that the stratosphere has cooled. In the tropics, new satellite techniques show the upper troposphere has warmed faster than the near-surface since 2001 *(medium confidence*). It is *very likely* that human influence, dominated by greenhouse gases, was the main driver of warming of the troposphere since the start of comprehensive satellite observations, and *extremely likely* that human influence, dominated by stratospheric ozone depletion, was the main driver of the cooling of the stratosphere. Most data sets show that lower stratospheric temperatures have stabilized since the mid-1990s, with no significant cooling over the last 20 years (*medium confidence*). {2.3.1, 3.3.1}

B.2.3 Several aspects of atmospheric circulation have *likely* changed since the 1980s. The tropical belt has *very likely* widened and intensified. There is *medium confidence* that greenhouse gas increases and stratospheric ozone depletion have contributed to this poleward expansion in the Southern Hemisphere. Extratropical storm tracks have *likely* shifted poleward. There is *high confidence* that stratospheric ozone depletion and human-induced increases in greenhouse gases have contributed to the observed poleward shift of the Southern Hemisphere jet in austral summer. It is *likely* that the northern stratospheric vortex has weakened. {2.3.1, 3.3.3, 3.7.2, 8.2.2, 8.3.2}

B.2.4 Near-surface specific humidity has *likely* increased over the ocean and *very likely* increased over land since at least the 1970s. Globally averaged, land precipitation has *likely* increased since 1950, with a faster increase since the 1990s (*medium confidence)*. It is *likely* that human influence has contributed to observed large-scale precipitation changes since 1950. There is *medium confidence* that rainfall over the wet regions of the tropics has increased due to enhanced greenhouse gas forcing and that ozone depletion has increased precipitation over the Southern Ocean and decreased it over southern midlatitudes during austral summer. There is *medium confidence* that trends in potential evaporation have exceeded trends in precipitation in some regions and seasons. {2.3.1, 3.3.2, 3.3.3, 8.3.1}

B.2.5 It is *very likely* that Northern Hemispheric anthropogenic aerosols have caused a weakening of the regional monsoon circulations in South Asia, East Asia and West Africa during the second half of the 20th century, thereby offsetting a strengthening monsoon precipitation in response to greenhouse gases-induced warming. There is *medium confidence* that the recent partial recovery in intensity of monsoon precipitation over West Africa is related to greenhouse gases increases and the transition from a decline to a partial recovery in surface solar radiation due to an overall radiative effect of anthropogenic aerosols. {2.3.1, 3.3.2, 3.3.3, 8.3.1, 8.3.2, Box 8.1}

[START FIGURE SPM.3 HERE]

This figure shows the contributions of different forcing agents to observed global surface temperature changes.

Figure SPM.3: Left panel shows global surface air temperature (GSAT) in observations (black), simulations with human and natural forcings (orange), well-mixed greenhouse gases only (grey), aerosols and other human forcings (blue), and natural forcings only (green) in CMIP6 models (solid lines show the mean and shading shows the 5-95% range) and in an emulator (dashed lines show the median). Right panel compares the observed warming in 2010-2019 relative to 1850-1900 with the assessed ranges attributable to net human influence (red), well-mixed greenhouse gases (grey), other human forcings (blue), and natural forcings (green). Shaded bars show the mid-points of the assessed ranges. Grey arrows show the median warming contributions from individual greenhouse gases, derived based on assessed ERF changes and an emulator. Similarly blue arrows show the contributions from other anthropogenic forcings, where the arrow labelled 'other' represents the net effects of black carbon on snow, contrails and stratospheric water vapour, the arrow labelled 'LUC' represents the physical effects of land-use change, and the green arrow represents the net effects of solar and volcanic forcing. Note that the sums of the individual forcing contributions based on the emulator do not agree exactly with the centre of the assessed ranges for each group of forcings, which draw on multiple lines of evidence, but they are consistent to within the uncertainties. {Figure TS.13}

[END FIGURE SPM.3 HERE]

[START FIGURE SPM.4 HERE]

Figure SPM.4: This figure shows how global temperatures have changed since 1850 and in a longer-term context. (a) Global mean surface temperature during the past 2000 years (median multi-method reconstruction (black line), with 2.5th and 97.5th percentiles of the ensemble members (grey bands)). The mean global ground surface temperature reconstructed from borehole temperature profiles (gold line), and the average of three instrumental-based datasets extending to 1850 (red line) are also shown for comparison. Large circles along left edge are best estimates for global mean temperature (bars are ± 2 SD) for mid-Holocene (around 6000 years ago), last glacial maximum (around 20,000 years ago), and last interglacial period (around 125,000 years ago). (b) Combined land and sea surface temperatures based on five different datasets. Top panel: annually resolved temperatures. Bottom panel: decadal mean values. Grey shading in both panels shows the uncertainty associated with one of the datasets (HadCRUTv5). All temperatures are anomalies relative to 1850-1900. {2.3.1, TS.12}

[END FIGURE SPM.4 HERE]

[START FIGURE SPM.5 HERE]

The purpose of this figure shows how global temperatures have changed since 1850 and in a longer-term context.

Figure SPM.5: Trends in surface temperatures from HadCRUTv5 (left panels) and precipitation from GPCCv8 (right panels) with statistical significance denoted by crosses. Top panels denote trends over the early 20th century and bottom panels denote trends over the more recent 40 years. Data are only shown where sufficient data exists over the entire time span of each panel. {Figure 2.11, Figure 2.14, TS.12, TS.19}

[END FIGURE SPM.5 HERE]

B.3 Ocean

The observed changes in the ocean are unprecedented over recent millennia. More than 90% of the energy added to the climate system as a result of greenhouse gas emissions is absorbed by the ocean, leading to sea level rise through thermal expansion. Confidence in the assessment of the planetary energy gain is higher than in AR5 through consistent closure of the global sea level budget for the period 1971–2018. There is *high confidence* that present surface ocean pH observations are at their lowest values for the past two million years and it is *virtually certain* that ocean acidification is predominantly driven by the ocean uptake of anthropogenic carbon dioxide. It is *virtually certain* that large-scale changes in near-surface and subsurface salinity patterns (fresh get fresher, saltier get saltier) have occurred since at least 1950, adding to the observational evidence for an intensification of the water cycle. (Figure SPM.1, Figure SPM.2) {2.3, 3.5, 4.3, 5.3, 5.4, 7.2, 9.2, 9.3, 9.6, Figure 5.20, Figure 5.21, Table 7.1, Box 7.2, Cross-Chapter Box 9.2, TS2.3}

B.3.1 The observed increase in ocean heat content (OHC) represents more than 90% of the observed total Earth system warming from greenhouse gases. It is *extremely likely* that anthropogenic forcing has made a substantial contribution to the OHC increase over the historical period. Observations show that warming extends throughout the entire water column (*high confidence*), with 65% estimated to be taken up by the upper (0–700 m), 20% by the intermediate (700–2000 m) and 15% by the deep (>2000 m) layers. The surface changes are transmitted slowly to the depths through ocean circulation, leading to substantial commitment in future sea-level rise and ocean uptake of heat and anthropogenic carbon over decades to centuries. Over years to decades, regional patterns of OHC change tend to be dominated by internal variability in ocean circulation. {3.5, 4.3.2, 5.4, 7.2.2, 9.2, 9.6, Table 7.1, Box 7.2, Cross-Chapter Box 9.2, TS2.3.6}

B.3.2 Global mean sea level (GMSL) has risen by 0.19 m (*likely* 0.15–0.22 m) between 1900 and 2018, mostly from ocean thermal expansion and glacier melt. GMSL increased faster since 1900 than over any century during the last three millennia, and GMSL change has accelerated since the late 1960s (*high confidence*). It is *very likely* that anthropogenic forcings are the main driver of the observed GMSL rise since 1970. {2.3.3, 9.3.5}

B.3.3 Ocean acidification is strengthening as a result of the ocean continuing to take up 23 ± 6% of the global anthropogenic CO_2 emissions (*high confidence*). There is *high confidence* that upper layer ocean pH has declined since the early 20th century and *very high confidence* that surface pH values as low as today have not been experienced in the last two million years. Deoxygenation has occurred in the upper km of open ocean since 1970, alongside an expansion of the volume of oxygen minimum zones (*medium confidence*). {2.3.3, 2.3.4, 5.3.2, 5.3.3, Figure 5.20, Figure 5.21}

B.3.4 It is *extremely likely* that human influence has contributed to observed near-surface and subsurface oceanic salinity changes since the mid-20th century with spatial patterns that suggest an intensification of the water cycle (*high confidence*). Surface-intensified temperature and salinity changes have increased the stratification of the upper ocean at a rate of 5-20% per decade for the period 1970 to 2018 (*medium confidence*). {2.3.3, 2.3.4, 3.5, 5.3.2, 5.3.3, Figure 5.20, Figure 5.21}

B.3.5 Direct observations show that the Atlantic Meridional Overturning Circulation (AMOC) has weakened since about 2005 (*high confidence*). There is further evidence of AMOC weakening during the 20th century, but only with *low confidence* due to large method uncertainties and superposed multidecadal variations. The observational record is not long enough to determine if changes observed in the circulation of the Atlantic Ocean and Southern Ocean are due to internal variability, solar and volcanic forcing or a response to anthropogenic forcing. {2.3.3, 2.3.4, 3.5.4, 9.2}

B.4 Cryosphere

Over the past decades, pervasive loss of ice sheet and glacier mass, snow cover extent and sea-ice area, as well as increases of permafrost temperature have been observed. The Greenland Ice Sheet, Arctic sea ice and glaciers in many regions are now in states unprecedented over centuries or more (*high confidence*). Human influence was *very likely* the dominant cause of the observed reduction in Arctic sea ice, and it *very likely* contributed to the observed reductions of Northern Hemisphere spring snow cover and global glacier volume over the past four decades, and *likely* contributed to the surface melting of Greenland. Glacier and ice sheet loss has *likely* been the largest contributor to global sea-level rise since 1993. {2.3, 3.4, 7.4, 9.3, 9.4, 9.5}

B.4.1 Since about 1850, the Greenland Ice Sheet retreated overall (*high confidence*). It is *virtually certain* that the Greenland Ice Sheet has lost mass since the 1990s, *likely* contributing 10.6 ± 0.9 mm to global sea level rise over the period 1992–2018. It is *very likely* that the Antarctic Ice Sheet has lost mass since at least since the early 1990s, *likely* contributing 6.9 ± 1.4 mm to global sea-level rise over 1992–2018, and there is *medium confidence* that Antarctic ice sheet mass loss has accelerated over the last decades. {2.3, 3.4, 9.4}

B.4.2 Current glacier retreat is globally widespread and unprecedented since at least 1850 (*very high confidence*). Glaciers *likely* contributed 25 ± 18 mm to global sea-level rise between 1971 and 2016 and 17 ± 7 mm between 1993 and 2018. Global glacier mass loss since the last decades of the 20th century cannot be explained without human induced warming (*high confidence*). {2.3, 3.4, 9.5}

B.4.3 Arctic summer sea-ice area during the last decade was at its lowest since at least 1850, and humans have *very likely* caused at least half of the observed reduction in Arctic summer sea-ice area since 1979. There is *medium confidence* that current Arctic sea-ice loss is unprecedented over the past 1000 years. There is no significant trend in Antarctic sea-ice area for the period 1979 to 2018. {2.3, 3.4, 9.3}

B.4.4 Northern Hemisphere spring snow cover has decreased since at least 1978 (*very high confidence*) and seasonal snowfall has been delayed (*medium confidence*). There is *medium confidence* that this trend extends back to the 1920s and it is *very likely* that anthropogenic influence contributed to the reduction since 1950. Arctic and mountain permafrost has been lost over recent decades and, globally, permafrost has warmed by 0.3°C in the last decade (*medium confidence*). Permafrost warming is an Arctic-wide phenomenon, with widespread increases in temperatures in the upper 30 m over the past three to four decades (*high confidence*). {2.3, 3.4, 9.5}

B.4.5 Stronger surface warming at the poles than at low latitudes is a robust feature of the long-term response to greenhouse gas forcing and of observed climate changes in both hemispheres (*very high confidence*). The currently observed Arctic amplification is caused in part by surface albedo changes due to losses of snow cover and sea ice. {7.4}

B.5 Extremes

Changes in extremes are widespread since the 1950s[8], including a *virtually certain* increase in extreme air temperature and marine heatwaves (*high confidence*), intensification in extreme precipitation (*high confidence*), and increase in drought potential in the dry season when aggregated on the global scale (*high confidence*). There is *high confidence* that concurrent hot and dry extremes have increased on a global scale. There is *medium confidence* that wildfires have become more intense in some fire-prone regions, such as the Mediterranean, southwestern United States and Australia. It is *extremely likely* that human influence is the main contributor to the observed increase in the likelihood and severity of hot extremes, including marine heatwaves, and the observed decrease in the likelihood and severity of cold extremes. (Table SPM.1, Figure SPM6) {3.1, 8.3, 9.6, 11.2, 11.3, 11.6, 11.7, 11.8, 11.9, 12.4, Box 11.3, Box 11.4, Cross-Chapter Box 3.2, Cross-Chapter Box 9.1}

B.5.1 Evidence of observed changes in extremes and their attribution to human influence has strengthened since AR5, in particular for extreme precipitation, droughts, tropical cyclones, and compound extremes. There is evidence of an increase in the land area affected by concurrent extremes. The effects of increased greenhouse gas concentrations on extreme temperature are moderated, counteracted or amplified at the regional scale due to feedbacks or forcings such as regional land-use and land-cover changes or aerosols. Urbanization has exacerbated the effects of global warming in cities (*high confidence*) and modified precipitation patterns (*medium confidence*). Changes in aerosol concentrations have affected trends in hot extremes in some regions (e.g. Asia, Europe, North America), with the presence of aerosols leading to attenuated warming, in particular from 1950–1980. Irrigation and crop expansion have attenuated increases in summer hot extremes in some regions, such as the central North America (*medium confidence*). {3.1, 11.1, 11.3, 11.4, 11.5, 11.6, 11.7, 11.8, Box 11.3, 12.4.10, Cross Chapter Box 3.2}

B.5.2 It is *virtually certain* that there has been an increase in the likelihood and severity of hot extremes and a decrease in the likelihood and severity of cold extremes on the global scale since 1950. Trends in temperature extremes on land are generally larger (by about 50% to 200%) than those in global mean temperature, due to larger warming on land and additional feedback effects (*high confidence*). It is *extremely likely* that human influence is the main contributor to the observed increase in the likelihood and severity of hot extremes and the observed decrease in the likelihood and severity of cold extremes on global scales. The available evidence suggests that some recent hot extreme events could not have occurred without human influence (*medium confidence*). Extreme temperature trends on regional to continental scales are generally consistent with the global-scale trends (*high confidence*). {11.3, 11.9}

B.5.3 There is *high confidence* that heavy precipitation has intensified over land regions on a global scale. It is *likely* that, since 1950, the annual maximum amount of 1-day or 5-day precipitation over land has increased in more regions than it has decreased. It is *likely* that anthropogenic influence is the main cause of the observed intensification of heavy precipitation in land regions. There is *high confidence* that the seasonality of floods has changed in cold regions where snow-melt is involved. {11.4, 11.9, Cross Chapter Box 3.2}

[8] Reliable observations for extremes with global coverage are available only after 1950, and for this reason, assessments of past changes in extremes and their causes are also from 1950 onward, unless otherwise indicated.

B.5.4 There is *high confidence* that human influence has increased drought potential and increased the tendency towards drying in the dry season since the beginning of the 20th century, when aggregated on the global scale. There is *medium confidence* that some regions show more frequent hydrological droughts, predominantly southern Africa, southern North America, the Mediterranean region. There is *high confidence* that concurrent hot and dry extremes have increased on a global scale. {8.3.1, 11.6}

B.5.5 There is *medium confidence* that the probability of exceeding major tropical cyclone intensity (Category 3 or greater) has increased over the past 40 years. It is *very likely* that the average location of peak tropical cyclone wind intensity has migrated poleward in the western North Pacific Ocean since the 1940s. There is *medium confidence* that this cannot be explained by natural variability. There is *low confidence* for any trends in total global tropical cyclones frequency over the period of the instrumental record. {11.7.1}

[START FIGURE SPM.6 HERE]

The purpose of this figure is to show that we now have a lot of evidence that is attributed to anthropogenic climate change in different regions of the world for many different types of extreme events.

Figure SPM.6: The symbols depict types of extreme events for which one or more such events have been studied in the event attribution framework (see Appendix Table 11.A.1). The location of symbols does not indicate the places of the event occurrence as the symbols represent the synthesized assessment of all studies for the same type of events occurring in the region. The arrows indicate the direction of changes in the intensity and likelihood of the events due to anthropogenic climate change. A "mixed signal" indicates that different studies found different results regarding the direction of changes in magnitude and frequency, depending on the definition of the event. {11.2.5, Appendix Table 11.A.1, TS Cross-Section Box 2 Figure 2}

[END FIGURE SPM.6 HERE]

[START TABLE SPM.1 HERE]

Table SPM.1: Summary table on detected changes in extremes on global and continental scale. The purpose of this table is to provide an overview of observed changes in extremes and their attribution to human activity on large scales. Regional information is available in Table 11.1 of the underlying report. {Table 11.1, TS.7}

Phenomenon and direction of trend	Observed/detected trends since 1950 (for ca. +0.5°C global warming)	Human contribution to the observed trends since 1950 (for ca. +0.5°C global warming)
Warmer and/or more frequent hot days and nights over most land areas	*Virtually certain* on global scale	*Extremely likely* main contributor on global scale
Warmer and/or fewer cold days and nights over most land areas	*Virtually certain* on global scale	*Extremely likely* on global scale

Warm spells/heatwaves; Increases in frequency or intensity over most land areas	*Virtually certain* on global scale	*Very likely* on global scale
Cold spells/cold waves: Decreases in frequency or intensity over most land areas	*Virtually certain* on global scale	*Very likely* on global scale
Heavy precipitation events: increase in the frequency, intensity, and/or amount of heavy precipitation	*Likely* more regions with positive than negative trends	*Likely* main contributor to the observed intensification of heavy precipitation in land regions
Drought events: Increases in frequency, intensity and/or duration	*High confidence* that atmospheric evaporative demand displays a global drying tendency over continents, and that there is an observed tendency towards increased drying in the dry season since the beginning of the 20th century, when aggregated on global scale. *Medium confidence* that trends in potential evaporation have exceeded trends in precipitation in some regions and seasons.	*High confidence* that human influence has increased the drought potential and increased the tendency towards drying in the dry season since the beginning of the 20th century, when aggregated on the global scale
Floods and water logging: Increases in intensity and/or frequency	*Low confidence* in the majority of the world regions. *High confidence* in changes of flood seasonality, mostly in snow dominated regions.	*Low confidence* due to little evidence and high seasonality.
Increase in precipitation associated with tropical cyclones	*Low confidence* for detectable global trend in tropical cyclone (TC) rain rates, due to data limitations.	*Low confidence* for global TC rain rates. *Medium confidence* for increase in overall extreme rainfall events, which TCs contribute to. *High confidence* for global near-surface water vapor increases, which is expected to increase TC rainfall, all other things equal.

Increase in tropical cyclone intensity (maximum surface wind speed)	*Low confidence* in detection of longer-term (50 yr or more) global trends in tropical cyclone intensity due to data limitations. *Medium confidence* that the global probability of exceeding major intensity (Category 3 or greater) has increased since the late 1970s, based on homogenised data over the geostationary satellite period.	*Low confidence* for longer-term global changes in tropical cyclone intensity due to data limitations and lack of detection. *Medium confidence* that the global increase since the 1970s is not explained by natural variability, based on agreement with theoretical expectations and robust support from numerical models under warming scenarios. *Medium confidence* that a reduction in anthropogenic aerosol forcing has contributed substantially to the observed increase in North Atlantic tropical cyclone intensity since the 1970s. *Low confidence* for direct role of greenhouse gas forcing.
Changes in frequency of tropical cyclones	*Low confidence* in any observed trends in total global TC frequency over any part of the instrumental record since the mid-19th century, based on a lack of observed trends during the satellite period and a lack of process understanding of the climate drivers of frequency.	*Low confidence* for global frequency. *Medium confidence* that a reduction in anthropogenic aerosol forcing has contributed substantially to the observed increase in North Atlantic tropical cyclone frequency since the 1970s. *Low confidence* for direct role of greenhouse gas forcing.
Tropical cyclone track changes	*Low confidence* in the observed global poleward expansion of TC lifetime-maximum intensity (LMI) since the 1980s due to data uncertainty. *Medium confidence* in the poleward LMI migration in the western North Pacific since the 1940s, based on higher quality data and agreement among different available regional data sources. *Low confidence* in observed global slowdown in TC translation speed since the 1940s due to data uncertainties and lack of model support. *Medium confidence* in the observed slowdown over the contiguous United States since 1900, based on confidence in the long-term data.	*Low confidence* for global poleward expansion of the location of LMI. *Medium confidence* for the migration in the western N. Pacific, based on a robust trend after regressing modes of inter-decadal variability from the time series, consistency with the independently-measured rate of tropical expansion and process understanding, and agreement with numerical models. *Medium confidence* for the slowdown over the US, based on the length of record and a robust trend after regressing modes of inter-decadal variability from the time series.
Severe convective storms (tornadoes, hail, rainfall, wind, lightning)	*Low confidence* in past trends in hail and winds and tornado activity due to short length of high-quality data records.	*Low confidence*.

Increase in compound events	*Medium confidence* that compound flooding risk has increased along the US coastline. *High confidence* that co-concurrent heatwaves and droughts are becoming more frequent under enhanced greenhouse gas forcing at global scale. *Medium confidence* that wildfires have become more intense and that their frequency has increased in some fire-prone regions.	*Low confidence* that human influences has contributed to changes in compound events leading to flooding. *High confidence* that human influence has increased the frequency of co-concurrent heatwaves and droughts. *Medium confidence* that human influence has increased wildfire occurrence in some regions.

[END TABLE SPM.1 HERE]

[START BOX SPM.2 HERE]

Box SPM.2: Scenarios and future climate system changes across timescales

Climate change projections require information about future emissions or concentrations of greenhouse gases and aerosols, changes in land use, and other anthropogenic forcings. This information can be provided by scenarios generated by internally consistent assumptions about socio-economic systems changing over the 21st century. Emissions from natural sources are either constant or evolve in response to changes in anthropogenic forcings or in response to projected climate change. Natural forcings such as changes in solar irradiance and volcanic eruptions are also explicitly taken into account. {1.6.1, 4.2.2}

Use of climate change scenarios in IPCC WGI AR6

In this report, a core set of five emission scenarios is used to explore climate change as simulated by Earth System Models run under the Sixth Phase of the Coupled Model Intercomparison Project (CMIP6). These five scenarios illustrate a range of possible climate futures and are labelled SSP1-1.9, SSP1-2.6, SSP2-4.5, SSP3-7.0, and SSP5-8.5[9]. This scenario set spans a range of radiative forcing levels that, at its lower end, is wider than the range of the Representative Concentration Pathways (RCPs) used in the AR5 assessment. In this report, the RCPs complement the core set of AR6 scenarios for assessments where no CMIP6-based results are available or for comparison to earlier IPCC reports. Since the RCPs are also labelled by the level of radiative forcing they reach in 2100, they can be directly related to the core set of AR6 scenarios. When projections extend beyond the 21st century, they are based on simple idealized assumptions about the post-2100 evolution of emissions or of radiative forcing that do not represent fully consistent socioeconomic scenarios. {1.6.1, Box 1.3, Cross-Chapter Box 1.5, TS.1.3.1, TS Cross-Section Box TS.1}

SSP1-1.9 represents the low end of radiative forcing outcomes found in scenarios in the literature and was initially designed to limit warming in 2100 to below 1.5°C. At the opposite end of the range, SSP5-8.5 represents the high end of the range of future pathways in the literature, with no climate policy implemented and a high reliance of carbon-intensive energy sources. SSP3-7.0 is a lower pathway that is also considered an unmitigated baseline scenario. SSP2-4.5 and SSP1-2.6 represent scenarios with incrementally stronger climate mitigation, where SSP1-2.6 was designed to limit warming to below 2°C. The full range and diversity of emissions scenarios with or without climate policies is assessed in WGIII. {1.6.1, Box 1.3, Cross-Chapter Box 1.5, TS.1.3.1, TS Cross-Section Box TS.1}

Air pollution control assumptions in the core set of scenarios are consistent with the scenarios' underlying socio-economic narratives. Control of air pollutants is considered to be strong in SSP1-1.9, SSP1-2.6 and SSP5-8.5 scenarios, medium in SSP2-4.5 and weak in SSP3-7.0. Combined with climate change mitigation measures, these air pollution controls are projected to lead to a strong decline of ozone precursor and aerosol emissions in the mid (2041–2060) to long term (2081–2100) in SSP1-1.9, SSP1-2.6 and SSP5-8.5, while they would follow current trends in SSP2-4.5, and see strong increases over the 21st century in SSP3-7.0. Methane emissions follow climate mitigation and decline rapidly in the SSP1-1.9 and SSP1-2.6 but do so only after 2070 in SSP5-8.5. {6.2, 6.6.1, TS1.3.1}

Scenario-based future climate system changes across timescales

Key findings of scenario-based climate model projections are summarized in Box SPM.2 Tables 1-3. Selected indicators of global climate change at 21st century reference time periods assessed in this report and beyond 2100, where relevant, are presented in Box SPM.2 Tables 1 and 2. The temporal evolution of these key variables is shown in SPM.C Figure 7. Key assessment conclusions are presented in Sections SPM.C and SPM.D.

Future projections are also assessed as a function of *global warming levels* (SPM Box.2 Figure 1), because

[9] Throughout this report, scenarios are referred to as SSPx-y, where "SSPx" refers to the Shared Socioeconomic Pathway or "SSP" describing the socio-economic trends underlying the scenario and "y" refers to the approximate level of radiative forcing resulting from the scenario in the year 2100.

of the close connection between the level of global warming and regional changes in extremes and many indices of climatic impact drivers (Section SPM.C). Finally, the near-linear relationship between *cumulative carbon emissions* (presented in Box SPM.2, Table 3) and projected warming, whose uncertainty quantification takes into account the additional climate effect of non-CO_2 forcers, offers an additional scenario- and path-independent approach to assess future projections and enables a direct link to questions related to specific temperature targets and remaining carbon budgets (Section SPM.D). {1.6.2, 1.6.3}

[START BOX SPM.2, TABLES 1-3 HERE]

The purpose of these tables is to summarize the scenario-based projection results for two global indicators, global mean temperature change and global mean sea level change, complemented by one inherent scenario property, global cumulative carbon emissions. Tables 1 (GSAT) and 3 (cumulative carbon emissions) connect the dimensions of integration used across chapters and Working Groups in the AR6.

[START BOX SPM.2, TABLE 1 HERE]

Box SPM.2, Table 1: Assessment results for GSAT change, based on multiple lines of evidence. The change is displayed in °C relative to the 1995–2014 reference period for selected time periods (near term 2021–2040, mid-term 2041–2060, and long-term 2081–2100), and as the time when certain temperature thresholds are crossed, relative to the period 1850–1900. The observed warming in 1995–2014 relative to 1850–1900 is 0.91°C (0.78–1.05°C) (Box TS.4, Table 1). Adding 0.91°C to the best estimate and the ranges for the selected time periods provides an approximation for the GSAT change relative to the 1850-1900 reference period. The timing of crossing a threshold is estimated for human-induced warming and does not include the uncertainty arising from natural variability. The table gives both the best estimate and, in parentheses, the *very likely* (5–95%) range. There is *high confidence* in the changes over the twenty-year periods relative to 1995–2014, which combine constrained CMIP6 projections and emulator results (Cross-Chapter Box 7.1). There is *medium confidence* in the timings when certain global warming levels are reached, which are based on a combination of emulator results and one set of constrained CMIP6 projections for SSP1-2.6, SSP2-4.5, and SSP5-8.5 but solely on emulator results for SSP1-1.9 and SSP3-7.0. An entry n.a. means that the global warming level is not attained during the period 2021–2100. GSAT estimates are assessed to be about 4% (2-7%) higher than equivalent GMST estimates. {4.3.1, Table 4.1, TS Cross-Section Box TS.1}

	Scenario	**Period 2021–2040 relative to 1995–2014**	**Period 2041–2060 relative to 1995–2014**	**Period 2081–2100 relative to 1995–2014**	**Timing of 1.5°C, relative to 1850–1900**	**Timing of 2°C, relative to 1850–1900**	**Timing of 3°C, relative to 1850–1900**	**Timing of 4°C, relative to 1850–1900**
Global Surface Air Temperature Change (ºC)	SSP1-1.9	0.7 (0.4, 0.9)	0.8 (0.5, 1.1) 0.9	0.6 (0.3, 0.9)	2028 (2022, n. a.)	n.a. (n.a., n.a.)	n.a. (n.a., n.a.)	n.a. (n.a., n.a.)
	SSP1-2.6	0.6 (0.4, 0.8)	0.9 (0.6, 1.2)	1.0 (0.6, 1.4)	2033 (2024, 2053)	n.a. (2047, n.a.)	n.a. (n.a., n.a.)	n.a. (n.a., n.a.)
	SSP2-4.5	0.7 (0.4, 0.9)	1.1 (0.8, 1.5)	1.9 (1.3, 2.5)	2031 (2024, 2042)	2050 (2040, 2073)	n.a. (2074, n.a.)	n.a. (n.a., n.a.)
	SSP3-7.0	0.7 (0.4, 0.9)	1.3 (0.9, 1.8)	2.9 (2.0, 3.8)	2029 (2023, 2038)	2046 (2036, 2060)	2074 (2058, 2098)	2100 (2079, n.a.)
	SSP5-8.5	0.7 (0.5, 1.0)	1.6 (1.1, 2.0)	3.6 (2.6, 4.7)	2028 (2022, 2036)	2042 (2035, 2051)	2064 (2054, 2078)	2082 (2069, 2100)

[END BOX SPM.2, TABLE 1 HERE]

[START BOX SPM.2, TABLE 2 HERE]

Box SPM.2, Table 2: Global mean sea-level projections for the five scenarios of the core set of this report. Numbers given are median values, (*likely*) and [*very likely*] ranges of the process-based model ensemble in metes for the specified time periods, relative to 1995-2014. Due to current limited availability of CMIP6 model runs, results for SSP1-1.9 are missing. Long-term sea level estimates will be added for FGD if available {9.3.6, Table 9.6, TS Cross-Section Box TS.1}

Sea Level Rise (m)	Scenario	Year 2040 (near-term) relative to 1995–2014	Year 2050 (mid-term) relative to 1995–2014	Year 2090 (long-term) relative to 1995–2014	Year 2100 relative to 1995–2014	Year 2150 relative to 1995–2014	Year 2300 relative to 1995–2014
	SSP1-1.9	--	--	--	--	--	--
	SSP1-2.6	0.14 (0.10--0.17) [0.08--0.20]	0.19 (0.15--0.23) [0.12--0.27]	0.39 (0.28--0.52) [0.19--0.65]	0.47 (0.33--0.64) [0.21--0.84]	--	--
	SSP2-4.5	0.14 (0.10--0.17) [0.08--0.19]	0.19 (0.15--0.24) [0.12--0.28]	0.45 (0.35--0.58) [0.26--0.71]	0.55 (0.40--0.71) [0.28--0.89]	--	--
	SSP3-7.0	0.14 (0.11--0.17) [0.08--0.20]	0.19 (0.15--0.24) [0.12--0.27]	0.51 (0.41--0.64) [0.33--0.75]	0.65 (0.51--0.81) [0.41--1.00]	--	--
	SSP5-8.5	0.14 (0.11--0.18) [0.08--0.22]	0.21 (0.16--0.26) [0.13--0.30]	0.59 (0.48--0.71) [0.39--0.83]	0.73 (0.60--0.90) [0.50--1.07]	--	--

[END BOX SPM.2, TABLE 2 HERE]

[START BOX SPM.2, TABLE 3 HERE]

Box SPM.2, Table 3: Global cumulative carbon emissions relative to 2015 in GtCO2 until the middle of three time periods and for the time of reaching 4 different warming levels under the five scenarios of the core set of this report. Numbers in columns 3-5 are derived from the scenario data base. The timing of crossing a threshold in columns 6-9 is estimated for human-induced warming and does not include the uncertainty arising from natural variability. Results given are for the best estimate year for each scenario (see Box SPM.2, Table 1). An entry n.a. means that the global warming level is not attained during the period 2021–2100. {1.6.1, Box 1.3, TS Cross-Section Boxes TS.1 and TS.2}

Illustrative Cumulative Carbon Emissions ($GtCO_2$)	Scenario	Year 2030 estimate relative to 2015	Year 2050 estimate relative to 2015	Year 2090 estimate relative to 2015	Estimate at 1.5°C, relative to 1850–1900 (best estimate only)	Estimate at 2°C, relative to 1850–1900 (best estimate only)	Estimate at 3°C, relative to 1850–1900 (best estimate only)	Estimate at 4°C, relative to 1850–1900 (best estimate only)
	SSP1-1.9	541	760	578	493	n.a.	n.a.	n.a.

	SSP1-2.6	607	1127	1279	706	n.a.	n.a.	n.a.
	SSP2-4.5	661	1539	2847	705	1539	n.a.	n.a.
	SSP3-7.0	744	1913	4724	691	1664	3530	5529
	SSP5-8.5	749	2144	6705	640	1518	3489	5663

[END BOX SPM.2, TABLE 3 HERE]

[START BOX SPM.2, FIGURE 1 HERE]

Box SPM.2, Figure 1: The purpose of this figure is to connect scenarios, scenario-based projections and warming levels. The figure synthesizes the dimensions of integration by providing a visual link between SSPs, annual CO_2 emissions, the assessed GSAT ranges for SSP scenarios for the end of the 21st century and the time periods at which the specific warming levels are reached. Combining ranges of projected temperature change and the time when particular warming levels are reached: time series of SSP-based annual CO_2 emissions from fossil fuel combustion and land use change for the core set of five illustrative SSP scenarios used in this report. SSP-based temperature projections for two time periods in the 21st century (vertical bars to the right of the panel). Note that the projected changes in GSAT are not based on raw model outputs, but on multiple and converging lines of evidence that enable the narrowing of the range of possible temperature outcomes. Adding 0.91°C to the best estimate and the ranges for the selected time periods provides an approximation to the 1850-1900 baseline (see Box TS.4, Table 1). Time when particular warming levels relative to 1850-1900 are reached in the SSPs (along the top axis, with circles under each warming level indicating best estimates for the individual scenarios. 5-95% uncertainty ranges will be added in FGD version). {1.6.1, Box 1.3, TS Cross-Section Boxes TS.1 and TS.2}

[END BOX SPM.2, FIGURE 1 HERE]

C. Our possible climate futures

PREAMBLE: *Climate projections explore a subset of possible futures through different human-induced emission pathways and using a diversity of models ranging from simple global mean surface temperature emulators to more comprehensive Earth System Models. While scenarios have a long history in IPCC, global warming levels are also useful to contrast our possible climate futures irrespectively of the time horizon at which the warming level is reached.*

C.1 Future global warming levels

Since AR5, significant progress from observational and paleoclimate constraints, together with improved climate modelling capabilities and understanding of climate feedbacks, provide a more accurate assessment of the global temperature response to future radiative forcing resulting from human activities. Global warming 1.5°C, neglecting the influence of natural internal variability, is estimated to occur around 2030, across all scenarios assessed in this report (*medium confidence*).. The assessed *likely* range of global mean surface air temperature over the period 2081–2100 is *very likely* to correspond to anomalies of 1.2°C-1.8°C compared to pre-industrial climate for SSP1-1.9, and of 2.9°C-4.7°C for SSP3-7.0. The magnitude of global warming by the end of the 21st century will be determined by future greenhouse gas emissions (*very high confidence*). (Figure SPM.7, SPM Box.2) {4.3, 4.4, 4.6, Table 4.6, Box 4.1, 5.6, 7.4, 7.5, Cross-chapter Box 2.3, TS Table TS.2}

C.1.1 The rate and magnitude of future global warming is determined by human emissions pathways, natural forcings (e.g., volcanic eruptions), global climate feedbacks, including carbon cycle feedbacks, and the storage of energy by the climate system. The climate response amplified by the net radiative feedback from the combined effect of changes in atmospheric water vapour, surface albedo and clouds, differences between atmospheric and surface warming, and non-CO_2 biogeochemical changes (*very high confidence*). The uncertainty range for the net cloud feedback has been halved since AR5, resulting in *high confidence* that this feedback amplifies global warming. {7.4}

C.1.2 A global surface air temperature warming level of 1.5°C relative to 1850–1900 is, in the near-term (2021–2041), *very likely* to be reached in scenarios SSP3-7.0 and SSP5-8.5, *likely* to be reached in scenarios SSP1-2.6 and SSP2-4.5, and *more likely than not* to be reached in Scenario SSP1-1.9 (*high confidence*).{2.3.1, 4.3.1, 4.4.1, Box 4.1, Cross-Chapter Box 2.3, TS Table TS.2}

*C.1.3 Global warming in 2081-2100 compared to 1995-2014 is very likely 0.3-0.9°C, 0.6–1.4°C, 1.3–2.5°C, 2.0-3.8°C and 2.6-4.7°C in the scenarios SSP1-1.9, SSP1-2.6, SSP2-4.5, SSP3-7.0 and SSP5-8.5, respectively. This corresponds respectively to global warming levels of 1.2-1.8°C, 1.5-2.3°C, 2.2-3.4°C, 2.9-4.7°C and 3.5-5.6°C compared to pre-industrial climate***,** *given the ca. 0.9°C global warming observed from 1850-1900 to 1995-2014. The magnitude in global warming by the end of the century is dominated by greenhouse gas emissions still to be emitted into the atmosphere, while uncertainty ranges for that period is dominated by the uncertainty in Equilibrium Climate Sensitivity (ECS) and Transient Climate Response (TCR) (very high confidence). (Box SPM.2) {4.3.4, Table 4.6, Cross-chapter Box 2.3}*

C.1.4 The ratio of global mean temperature increase to cumulative CO_2 emissions, referred to as the Transient Climate Response to Cumulative Carbon Emissions (TCRE), stays approximately constant until peak warming over the 21st century for emission pathways limiting global warming in the 1.5°C to 2°C range (*medium confidence*). The TCRE is *likely* in the 1.0-2.2°C per 1000 PgC range[10] (*high confidence*). This is a slightly narrower range than in the AR5 assessment due to a better integration of different lines of evidence. Additional Earth system feedbacks, such as permafrost thawing and changes in the land carbon sink, have the potential to weaken the linearity of the cumulative carbon-climate relationship. This could result in potentially higher warming, further warming after net zero CO_2 emissions are reached, or a path dependency of warming as a function of cumulative emissions of CO_2 (*low confidence*). We understand the processes well but models are inconclusive in their projections of the carbon cycle after net zero and how elements of the carbon cycle will interact and respond with global warming, e.g. permafrost thawing. (Figure SPM.7) {5.5.1}

C.1.5 For mid- and high-emissions scenarios it is *very likely* that oceanic and terrestrial sinks will continue to take up CO_2 throughout the 21st century. It is *very likely* that the rate of the uptake will weaken from the second part of the century due to emerging climate feedbacks. For low-emissions scenarios (SSP1-1.9, SSP1-2.6) that entail a decrease in atmospheric CO_2 concentration accelerated by deployment of carbon dioxide removal, it is *very likely* that carbon sinks will weaken in the near term (2020-2040) and become sources towards the end of the 21st century (*medium confidence*). Due to model response uncertainty there is *low confidence* in the timing of the sink-to-source transition in low-emissions scenarios, particularly for the land sink. (Figure SPM.7) {4.6.3, 5.6}

C.1.6 The equilibrium climate sensitivity (ECS) and transient climate response (TCR) are two measures that are strongly related to the magnitude of global warming projected by Earth System Models (Box SPM.1). Since AR5, new methods of using observations combined with an improved understanding of how climate feedbacks change with climate state leads to strong agreement on values of global climate sensitivity metrics across assessed lines of evidence and to a reduction in uncertainty ranges. The best estimate of ECS is 3°C, the *likely* range is 2.5° to 4.0°C and the *very likely* range is 2.0° to 5.0°C. It is *virtually certain* that ECS is larger than 1.5°C. The best estimate of TCR is 1.8°C, the *likely* range is 1.4° to 2.2°C and the *very likely* range is 1.2° to 2.4°C. {7.5}

C.1.7 The currently-available CMIP6 models have higher average ECS and TCR values than the CMIP5 models. Increased ECS and TCR in many models can be traced to changes in extra-tropical cloud feedbacks that have emerged from efforts to reduce biases in these clouds compared to satellite observations (*medium confidence*). ECS and TCR ranges from CMIP6 models however span the assessed *very likely* ranges, leading the models to project a range of future warming that is wider than the assessed warming range based on multiple lines of evidence. The CMIP6 models with the highest ECS and TCRs values provide insights into high-risk, low-likelihood futures, which cannot be excluded based on currently-available evidence. However, some are less consistent with observed recent changes in global warming. {7.5}

[10] Corresponding to XXX °C/GtCO2

[START FIGURE SPM.7 HERE]

The purpose of this figure is to highlight the models' ability to capture recent trends in key climate change indicators, the different climate futures associated with different emissions scenarios (thick lines), the uncertainties due to both intermodel spread and internal climate variability for a given emission scenario (shading), the irreversibility of the global mean sea level rise at the multi-century timescale, and the non-linear response of the carbon cycle to global warming.

Figure SPM.7: Observed and projected time series of changes in (a) Annual global mean near-surface air temperature (GSAT), (b) Annual global land precipitation, (c) September Arctic sea ice area, (d) Northern Hemisphere (NH) spring snow cover extent, (e) Annual sea level change (global mean and thermosteric contribution from warming alone), (f) Annual Global sea level beyond 2100 (note that the axes differ to those in (e), (f) Annual ocean carbon sink, (g) Annual land carbon sink. Note that projected changes in GSAT are not based on raw model outputs, but on multiple and converging lines of evidence that enable to narrow the range of possible temperature outcomes. Near-term, mid-term and long-term climate changes as defined in the AR6 are bounded by grey bars.

[END FIGURE SPM.7 HERE]

C.2 Future ocean, cryosphere and sea level changes

Since AR5, progress has been made in narrowing uncertainties in future glacier and ice sheet mass losses. Arctic and Antarctic sea-ice extent, glacier mass, snow cover extent, near-surface permafrost volume, and ocean pH are all projected to decrease in a warming world, while ocean surface temperature, ocean heat content and sea level are projected to increase (*high confidence*). For the Antarctic Ice Sheet, future mass loss is *likely*, although slight mass gain cannot be excluded under strong mitigation scenarios. There is *medium confidence* that at a global warming level of between 2°C and 3°C, the Greenland Ice Sheet will pass a threshold where long-term mass loss becomes irreversible over centennial timescales. All future warming scenarios show committed sea-level rise of several metres after two millennia, with ice sheets the dominant uncertainty on century timescales. (Figure SPM.7) {2.3, 5.3, 5.4, 9.2, 9.3, 9.4, 9.5, 9.6, 12.4, Atlas.7}

C.2.1 It is *virtually certain* that global mean sea surface temperature will continue to increase throughout the 21st century, resulting in the exceedance of many hazard thresholds relevant to marine ecosystems (*medium confidence*). The surface and subsurface ocean will continue to warm throughout the 21st century (*very high confidence*) and *likely* over one or two centuries beyond 2100, thereby contributing to emissions pathway-dependent sea-level rise. There is *high confidence* that de-oxygenation will continue throughout the 21st century, and that the ocean will further acidify as CO_2 levels continue to rise. Future ocean warming will favour the development of hypoxic or minimal oxygen zones, including *very likely* irreversible change to occur in the Southern Ocean by 2030 under all medium-to-high emissions scenarios. {2.3.3, 5.3.3, 5.4.8, 9.2.1, 9.2.2, 9.6.4, 12.4.8, Atlas.7}

C.2.2 There is *high confidence* that thawing terrestrial permafrost will lead to carbon release, but the timing, magnitude and relative partitioning between CO_2 and CH_4 emissions can be estimated only with *low confidence.* Global permafrost volume in the top 3 m will decrease by about 25±5% per °C for global warming levels up to 4°C (*medium confidence*), with delayed thawing of deeper layers. The projected cumulative CO_2 release from permafrost is 74 ± 48 $GtCO_2$ per degree of global warming by 2100 (*low confidence*). {5.4, 9.5}

C.2.3 Projected Arctic sea ice area, snow cover extent and near-surface permafrost volume losses are approximately proportional to future global warming levels, until the remaining snow or ice volume becomes a major limitation for further proportional decline. Ice sheets and glaciers respond more slowly, implying committed changes on decadal to centennial (glaciers) and centennial or longer (ice sheets) time scales and limited direct scaling of integrated mass loss with global warming levels. The Arctic Ocean is *likely* to become sea-ice free throughout September for the first time before 2050 for all emission scenarios (*high confidence*). If global warming remains below 2°C throughout the 21st century, the Arctic Ocean will *likely* remain partly sea-ice covered all year round in most years. (Figure SPM.7) {9.3, 9.4, 9.5}

C.2.4 It is *likely* that the Greenland ice sheet will contribute 0.07 (0.03 to 0.12) m and 0.13 (0.09-0.19) m to GMSL by 2100 under SSP1-2.6 and SSP5-8.5, respectively. For future warming levels exceeding 2 to 3°C, there is *medium confidence* that the Greenland Ice Sheet will pass a threshold where long-term mass loss becomes irreversible over centennial timescales. It is *likely* that the Antarctic ice sheet will contribute 0.12 (0.00-0.26) m to GMSL by 2100 with little scenario dependence, but there is deep uncertainty regarding the Antarctic contribution under the high emissions scenarios. Globally, glaciers will diminish even if climate stabilizes (*very high confidence*) and are *likely* to contribute 0.07-0.11 m and 0.11-0.18 m to GMSL by 2100 under SSP1-2.6 and SSP5-8.5, respectively. {9.4, 9.5, 9.6}

C.2.5 It is *virtually certain* that GMSL will continue to rise through 2100 and beyond. GMSL is *likely* to increase by 0.33-0.64 m under SSP1-2.6, 0.40-0.71 m under SSP2-4.5, 0.51-0.81 m under SSP3-7, and 0.60-0.90 m under SSP5-8.5 between 1995-2014 and 2100. GMSL is *extremely unlikely* to increase by less than 0.2 m or more than 0.9 m by 2100 under SSP1-2.6 and SSP 2-4.5. GMSL rise due to thermal expansion, glacier melt, and Greenland ice sheet melt are all highly dependent on emissions scenario after 2050. In pathways leading to about 2°C of warming, GMSL rise is *likely* to be 0.33-0.65 m between 1995-2014 and 2100. The committed rise in GMSL after two millennia will be 1 to 3 m per °C peak warming (*low confidence*). (SPM Box.2) {9.6}

C.3 Large-scale warming patterns and circulation changes

Surface and atmospheric warming patterns and circulation changes are robust across scenarios and time horizons (*high confidence*), with a higher surface warming over land than ocean (*virtually certain*) and a strong amplification of surface warming in the Arctic (*high confidence*) across the 21st century. Summer-time warming in the mid-latitudes, including for hot extremes, will *very likely* be substantially larger than global mean warming. Changes in both tropical and extratropical atmospheric circulation, which affect regional precipitation patterns, are *very likel*y driven by the slowly evolving surface warming pattern and the fast atmospheric adjustment to the CO_2 radiative forcing. (Figure SPM.8, SPM Box.3) {4.2, 4.4, 4.5, 4.7, 7.4, 8.2, 8.4, 8.5, 9.2, 11.3, Atlas.5, Atlas.7}

C.3.1 There is improved understanding of the large-scale spatial patterns of temperature and circulation changes in response to global warming since the AR5. The amplification of land surface warming is more pronounced in the boreal winter high-latitudes and in the summertime mid-latitudes associated to regional feedbacks (e.g., snow and soil moisture) (*high confidence*). In most land regions changes in mean and extreme temperatures scale linearly with global warming. {4.5.1, 8.2.2, 11.2, 11.3, Atlas.7}

C.3.2 Warming in some regions that have historically warmed slowly or slightly cooled will eventually emerge and increase on centennial time-scale due to slowly responding ocean. It is expected that future surface warming will increase over the eastern Pacific Ocean (*medium confidence*) and Southern Ocean (*high confidence*) on centennial timescales. There is *high confidence* that Antarctic amplification will emerge as the Southern Ocean surface warms on centennial timescales, although there is only *low confidence* in this feature emerging this century. {4.5.2, 7.4.4, 7.4.4, 9.2.1, Atlas.7}

C.3.3 Projected changes in spatial warming contrasts will be associated with widespread changes in large-scale atmospheric circulation, also driven by atmospheric adjustments to the radiative forcings (*high confidence*). Global models project a weakening of the Northern Hemisphere monsoon circulation (*high confidence*) despite regional disparities, and an overall poleward shift of the extratropical jets, in all emissions scenarios but not necessarily proportional to global warming given the complex interplay between different drivers and timescales (*medium confidence*). {4.7.4, 8.2, 8.4.2}

C.3.4 It is *very likely* that the magnitude of the main modes of intraseasonal to interannual variability (e.g., Madden-Julian Oscillation and El Niño-Southern Oscillation (ENSO) in the tropics, annular modes and North Atlantic Oscillation in the extratropics) will not decrease substantially before 2100. It is *very likely* that the amplitude of ENSO rainfall variability will increase in the latter half of the 21st century (*high confidence*), regardless of amplitude changes in ENSO sea surface temperature variability and there is *medium confidence* that associated regional precipitation impacts will be enhanced over land. {4.3.3, 4.5.3, 8.4.2}

C.3.5 Internal variability will continue to exert a substantial influence on climate, especially in the near-term and at the regional scale (*high confidence*). Modes of decadal to multi-decadal variability will drive departures from the human-caused large-scale circulation response, which can temporarily exacerbate or mitigate regional warming rates, irrespectively of the SSP scenario. There is however *high confidence* that initialized climate predictions can be used to reduce the uncertainty in near-term temperature changes, on both ocean basin-wide and continental scales. {4.2.3, 8.5.2}

[START FIGURE SPM.8 HERE]

The purpose of the figure is to show the regional distribution of changes across a range of indicators, as a function of warming level. It highlights that even small changes in global warming lead to large changes in extremes.

Figure SPM.8: Global maps of projected changes at increasing global warming levels above 1850-1900 levels in (from top to bottom) annual mean temperature, daytime temperature of annual warmest day, annual exceedance of bias-adjusted (using quantile delta mapping) warmest daytime temperature (TX) over 35°C, annual mean precipitation, annual maximum daily precipitation, and annual maximum of consecutive dry days for 1.5°C (left), 2°C (middle) and 4°C (right) global surface air temperature (GSAT) above 1850-1900. {TS Cross-Section Box 2 Figure 1}.

[END FIGURE SPM.8 HERE]

C.4 Future changes of the water cycle

Since the AR5, growing evidence suggests that future water cycle changes will include large regional changes in seasonality, variability and extremes (*high confidence*). Water cycle variability over land will overall increase the frequency and severity of both dry and wet extremes (*medium confidence*). There is *high confidence* that increasing atmospheric evaporative demand will lead to further drying tendencies in some regions under higher global warming. Global and annual mean precipitation and evapotranspiration will increase over land (*high confidence*), but water cycle changes will mostly manifest as enhanced spatial and seasonal contrasts between dry and wet regimes (*high confidence*). These changes are increasingly dominated by the response to increased greenhouse gas concentrations, although other anthropogenic and natural forcings can still alter the near-term, regional hydrological responses (*high confidence*). (Figure SPM.7, Figure SPM.8) {4.3, 4.4, 4.5, 5.2, 5.4, 8.2, 8.4, 8.5, 8.6, 11.4, 11.5, 11.6, Box 11.2, Box SPM.3}

C.4.1 Paleoclimate studies show a water cycle response to past perturbations of the Earth's energy budget (*high confidence*). Based on process understanding and model projections, it is *virtually certain* that global mean precipitation and evaporation will increase with global warming. Over land, mean precipitation will *likely* increase by 1-3% per °C for the SSP5-8.5 scenario. Most water cycle changes will increase in magnitude with global warming, although their scaling is generally less linear compared to temperature increases, due to the larger relative influence of atmospheric adjustment to radiative forcings and, therefore, to emissions pathways (*medium confidence*). {4.3, 8.2, 8.5, 11.4, 11.5, 11.6}

C.4.2 Future changes in monsoon rainfall will exhibit regional contrasts. Despite a projected overall slowdown of the global monsoon circulation, monsoon rainfall will increase globally although more strongly in the Northern Hemisphere. Global land and high-latitude precipitation will increase with global warming. Regional and seasonal mean precipitation changes are driven by atmospheric circulation and moisture content changes and are modulated by regional land surface forcings and feedbacks. (*high confidence*). (Box SPM.3) {4.4, 4.5.1, 8.2, 8.4, 11.6, Box 11.2}

C.4.3 Globally, annual mean and daily precipitation over land are projected to increase with global warming, causing an overall increase in runoff, which will be region- and season-dependent. The amplitude of the seasonal cycle of precipitation, runoff, streamflow and water availability will increase over many regions. Earlier snowmelt will bring forward the timing of peak streamflow and reduce summer streamflow. (*high confidence*). (Box SPM.3) {8.4}

C.4.4 There is *high confidence* that increasing atmospheric evaporative demand will lead to further drying tendencies in some regions under higher global warming. Due to increased land surface temperatures, evapotranspiration will increase with global warming, resulting in soil drying in water-limited regions (*high confidence)*. Arid areas are projected to expand towards the midlatitudes due to shifts in large-scale atmospheric circulation and regional land surface feedbacks (*medium confidence*). (Box SPM.3) {8.4, 11.6}

C.4.5 Intraseasonal precipitation variability is projected to increase in many regions with global warming due to less frequent but heavier precipitation events (*high confidence*). Interannual variability of precipitation and runoff over land is projected to increase faster than the equivalent seasonal mean changes, when spatially averaged in the tropics and in the summer extratropics of both hemispheres (*medium confidence*). Decadal to multi-decadal internal variability strongly affects near-term water cycle responses for all emission scenarios, especially those related to regional summer monsoons and winter mid-latitude storm tracks (*medium confidence*). (Box SPM.3) {4.4, 4.5, 8.4, 8.5, 11.6}

C.4.6 Climate variability and emerging limitations on vegetation productivity by water availability will gradually reduce the positive effects of warming on ecosystem productivity in drying areas (*medium confidence*). Increasing atmospheric CO_2 will generally increase water-use efficiency of plants (*high confidence*) and would partly counteract water losses from rising evapotranspiration in a warmer climate (*medium confidence*). {5.2.1, 5.4.1, 5.4.3, 8.2.3, 8.5.1, 11.6.1}

C.5 Future changes in extremes and climatic impact drivers

Projected changes in the magnitude of regional temperature and precipitation extremes are *very likely* proportional to global warming. An additional half degree of global warming would cause further detectable changes in temperature extremes (*virtually certain*) and in precipitation extremes (*very likely*) at the global scale. Warm extremes are projected to become more frequent (*virtually certain*), cold extremes less frequent (*extremely likely*) and precipitation extremes more frequent in most locations (*very likely*). The frequency and severity of prolonged negative anomalies in precipitation, soil moisture, and streamflow are projected to increase in some regions (*medium confidence*). The highest category tropical cyclones will be associated with increased maximum wind speed and precipitation with increasing warming levels (*high confidence*). Concurrent extreme events affecting similar sectors in different regions will become more frequent (*high confidence*). (Figure SPM.8, Figure SPM.9, Table SPM.2, Box SPM.3) {11.3, 11.4, 11.7, 11.8, Box 11.4, 12.4}

C.5.1 It is *virtually certain that a*n additional half degree of global warming causes further detectable changes in temperature extremes and *very likely* for precipitation extremes at the global scale. It is *likely* that the frequency of rarer temperature and precipitation extremes will increase more than that of less rare events under higher warming. (Box SPM.3) {11.8, Box 11.4}

C.5.2 It is *virtually c*ertain that further increases in the likelihood and severity of hot extremes and decreases in the likelihood and severity of cold extremes will occur throughout the 21st century. It is *virtually certain* that the number of hot days and hot nights, as well as the length, frequency, and/or intensity of warm spells or heat waves will increase over most land areas. There is *high confidence* that many regions will experience heat stress conditions above critical thresholds for health, agriculture and other sectors. It is *very likely* that marine heat waves will increase in frequency, duration, spatial extent and intensity in all ocean basins. (Figure SPM.9, Box SPM.3) {11.3, 11.9, 12.4, Cross-Chapter Box 9.1}

C.5.3 Globally averaged over land, the intensity of extreme precipitation will *very likely* increase proportionally with global warming. The average and maximum rain rates associated with tropical and extratropical cyclones, atmospheric rivers and severe convective storms will increase as atmospheric water vapour increases with global warming. The magnitude of extreme precipitation is projected to increase by approximately 7% per 1°C of global warming. Flood potential in urban areas where extreme precipitation is projected to increase, especially at high global warming levels. (*high confidence*) (Figure SPM.9) {11.4, 11.5, 11.7}

C.5.4 The frequency and severity of prolonged negative anomalies in precipitation, soil moisture, and streamflow are projected to increase in some regions (*medium confidence*). Increasing aridity and variability are projected to drive an enhanced frequency and severity of droughts in midlatitude regions in the Northern and Southern Hemisphere (*medium confidence*). Projections of relative soil moisture deficits show stronger severity than projections of relative precipitation deficits in drought areas (*medium confidence*). These projections are strongly dependent on the warming scenario considered, with stronger drought trends for higher warming levels, even for changes as small as 0.5°C in global warming (*high confidence)*. Some regions with humid or transitional climate characteristics in the 20th century are projected to become drier (*medium confidence*). (Box SPM.3) {11.6, 8.4}

C.5.5 Average peak tropical cyclone wind speeds and the proportion of Category 4-5 tropical cyclones will increase globally with global warming (*high confidence*). The average location where tropical cyclones reach their maximum wind intensity will migrate poleward in the western North Pacific Ocean. The global frequency of tropical cyclones over all categories will decrease or remain unchanged. The frequency of springtime severe convective storms will increase, leading to a lengthening of the severe convective storm season. (*medium confidence*) {11.7.1, 11.7.2, 11.7.3}

C.5.6 The frequency of current 1% probability extreme sea level events will increase with continued global warming. Relative sea level rise is *very likely* to continue throughout the 21st century, contributing to increased coastal flooding in low-lying coastal areas and coastline recession along most sandy coasts. (*high confidence*) {9.6.3, 12.4}

C.5.7 Concurrent extreme events, affecting similar sectors in different regions, would become more frequent above 2°C of global warming (*high confidence*). The frequency of concurrent heatwaves and droughts will continue to increase under higher levels of global warming (*high confidence*). Compound coastal flood risk (storm surge, extreme rainfall and/or river flow) will continue to increase in some regions due to both sea level rise and increases in heavy precipitation (*medium confidence*). (SPM Box.3) {11.8, Box 11.4}

[START TABLE SPM.2 HERE]

Table SPM.2: Synthesis Table on projected changes in extremes. This Table summarizes the main AR6 assessments on extremes at 1.5°C and 3°C of global warming. Regional information is available in Table 11.1 of the underlying report. {Table 11.2, TS.8}

Phenomenon and direction of trend	Projected changes at +1.5°C global warming (unless specified: compared to pre-industrial conditions)	Projected changes at +3°C global warming (unless specified: compared to pre-industrial conditions)

Warmer and/or more frequent hot days and nights over most land areas	*Virtually certain* on global scale *Extremely likely* on all continents *Virtually certain* larger increases at +1.5°C compared to +1°C in most land regions Frequency of very hot days (1% probability) ~3 times larger on global scale compared to present (*high confidence*; Box on Global warming levels) Decadal average warming of hottest days of up to +3°C in mid-latitudes (*medium confidence*)	*Virtually certain* on global scale *Extremely likely* on all continents *Virtually certain* larger increases at +3°C compared to +2°C in most land regions Decadal average warming of hottest days of up to +6°C in mid-latitudes (*medium confidence*)
Warmer and/or fewer cold days and nights over most land areas	*Virtually certain* on global scale *Extremely likely* on all continents *High confidence* in larger decreases at +1.5°C compared to +1°C in most land regions Warming of coldest nights of up to +4.5°C (e.g. Arctic) (*medium confidence*)	*Virtually certain* on global scale *Extremely likely* on all continents *Extremely likely* larger decreases at +3°C compared to +2°C in most land regions Warming of coldest nights of up to +9°C (e.g. Arctic) (*medium confidence*)
Warm spells/heatwaves; frequency and/or duration increases over most land areas	*Virtually certain* on global scale *Extremely likely on* all continents	*Virtually certain* on global scale *Extremely likely* on all continents
Increase in marine heatwave (MHW) frequency, intensity and duration	*Very likely* in all ocean basins, but with differential magnitudes in space. *High confidence* that a permanent MHW state can be avoided.	*Very likely* in all ocean basins, but with differential magnitudes in space. *Medium confidence* of a near permanent MHW state in many parts of the ocean
Cold spells/cold waves: Decreases in frequency, intensity and/or duration over most land areas	*Very likely* on global scale	*Very likely* on global scale
Heavy precipitation events: increase in the frequency, intensity, and/or amount of heavy precipitation	*Very likely* on global scale *Very likely* increase at +1.5°C compared to +1°C on global scale	*Very likely* on global scale *Very likely* in most continents but *low confidence* in Australasia, Central and South America *Very likely* increase at +3°C compared to +2°C on global scale

Increases in floods and water logging	*Medium confidence* in a larger fraction of land area affected by flood hazard at global scale compared pre-industrial time and compared to present	*High confidence that* flood hazard would be even more widespread at +3°C compared to +2°C given projected changes in heavy precipitation; in part lack of literature to quantitatively assess projected changes.
Increases in intensity and/or duration of drought events	*High confidence* that atmospheric evaporative demand will continue to increase and lead to further drying tendencies in some regions *Medium confidence* in increase in drought probability in subtropical regions	*High confidence* that atmospheric evaporative demand will continue to increase and lead to further drying tendencies in some regions *Medium confidence* in increase in drought probability in subtropical regions, with higher probability of intense/frequent droughts than at 2°C of global warming ; *Medium confidence* in expansion of drought probability outside these regions given increased radiative forcing, with probability of intense droughts being higher than at 2°C of global warming
Increase in precipitation associated with tropical cyclones (TC)	*High confidence* in a projected increase of TC rain rates at the global scale. *Medium confidence* that rain rates will increase in every basin.	*High confidence* in a projected increase of TC rain rates at the global scale. *Medium confidence* that rain rates will increase in every basin.
Increase in mean tropical cyclone lifetime- maximum wind speed (intensity)	*High confidence* for a global increase.	*High confidence* for a global increase.
Changes in frequency of tropical cyclones	*High* confidence for an increase in the proportion of TCs that reach the strongest (Category 4-5) levels. *Medium confidence* for decrease or no change in global frequency of all TCs.	*High confidence* for an increase in the proportion of TCs that reach the strongest (Category 4-5) levels. *Medium confidence* for decrease or no change in global frequency of all TCs.
Changes in tropical cyclone track	*Medium confidence* for poleward migration in the western North Pacific Ocean.	*Medium confidence* for poleward migration in the western North Pacific Ocean.
Severe convective storms	*Medium confidence* that the frequency of severe convective storms increases in the spring with enhancement of Convective Available Potential Energy, leading extension of seasons of occurrence of severe convective storms. *High confidence* of future intensification of precipitation associated with severe convective storms.	
Increase in extreme sea levels	*High confidence* for substantial frequency increases in the current 1% annual probability event.	*High confidence* for further frequency increases in the current 1% annual probability event.

Increase in compound events (frequency, intensity)	*High confidence* that co-concurrent heatwaves and droughts will continue to increase under higher levels of global warming, with higher frequency/intensity with every additional 0.5°C of global warming. *Medium confidence* that humid heatwaves will continue to increase under higher levels of global warming, with higher frequency/intensity with every additional 0.5°C of global warming. *Medium confidence* that compound flooding at the coastal zone will increase under higher levels of global warming, with higher frequency/intensity with every additional +0.5°C of global warming.

[END TABLE SPM.2 HERE]

[START FIGURE SPM.9 HERE]

Figure SPM.9: Projected changes in the magnitude and frequency of extreme temperature and precipitation under different global warming levels. A, C: Global land median changes in the 50-year return values of annual maximum daily maximum temperature (A) and annual maximum one-day precipitation (C) with respect to global warming level in the CMIP6 multi-model ensemble simulations under different future forcing scenarios. The black solid lines mark the median regression lines of the scatter points, while the grey envelopes bound the 5-95% regression lines of the scatter points. B, D: Global land median changes in the frequencies of hottest day temperature (B) and heaviest day rainfall amount (D) that occurs once in 10 year (10-year event) or once in 50 years (50-year event) on average in the 1°C warming climate under different warming levels. The average waiting time for such events to occur is marked on the right side of the plots. The horizontal line and the height of the box represent median and interquartile range of the changes and the whiskers extend to the full range of the change estimated from simulations by different CMIP6 models under different SSP scenarios. Warming level is defined as global mean near surface air temperature relative to 1850-1990 mean. The figure highlights that: 1) the projected changes in the magnitude of extreme temperature and extreme precipitation increase with global warming level near-linearly, independent of SSP scenarios; 2) projected changes in the frequency increases with global warming level non-linearly; 3) increase in the frequency is larger for less frequent events. [Placeholder: The figure is based on one run per model from all models participating in CMIP6 whose relevant simulations were available at the time of analysis, which will be re-computed for FGD with large-ensemble model runs of CMIP6 models to obtained more robust estimate]

[END FIGURE SPM.9 HERE]

C.6 Other plausible future changes, including low-likelihood, high-impact climate trajectories

The likelihood for unforeseen low-likelihood, high-impact events related to extremes and tipping points is larger for global warming above 1.5ºC and there can be abrupt changes in the water and carbon cycles at the regional scale (*low confidence*). Major volcanic eruptions represent a source of irreducible uncertainty for near-term projections. The short-lived climate effects following eruptions are however well understood (*high confidence*). {2.3, 4.3, 4.4, 4.7, 4.8, 5.1, 5.2, 5.4, 7.5, 8.5, 8.6, 9.2, 9.4, 10.5, 11.2, 11.3, 11.6, Table 4.9, Figure 4.19}

C.6.1 Storylines can be built to investigate low-probability high-impact scenarios, for instance associated with high ECS and TCR values, contrasted but plausible large-scale circulation changes, or strong regional climate feedbacks. Storylines leading to high global warming are *virtually certain* to be associated with large changes in the frequency and intensity of very rare extreme temperature and precipitation events. {4.8, 7.5, 10.5.3, 11.2, 11.3, 11.4}

C.6.2 Abrupt regional changes in the water and carbon cycles cannot be excluded at high global warming levels (*low confidence*). Paleo records do not provide strong support for abrupt changes in the carbon cycle for global warming below 2ºC (*low confidence*). Deforestation and global warming raise the probability that the Amazon will cross a tipping point into a dry state, although there is *low confidence* that such a change will occur before 2100. Loss of permafrost carbon is *likely* irreversible, but its magnitude is still highly uncertain at high warming levels. Most Earth System Models still neglect or poorly represent some carbon-climate feedbacks, such as those associated with permafrost, fires, droughts and vegetation mortality. {4.8, 5.1, 5.2, 5.4, 8.6, 11.6}

C.6.3 Potential abrupt changes in the ocean and cryosphere include an AMOC collapse or a destabilization of Greenland and Antarctic ice sheets. Although it is *unlikely* that an abrupt collapse of the AMOC will occur during the 21st century, such a collapse cannot be ruled out after 2100 (*low confidence).* {2.3, 4.3.2, 8.6.1, 9.2.3}

C.6.4 There is deep uncertainty regarding the Antarctic contribution to global mean sea level rise under the high emissions scenarios. {4.7.3, 9.2.3, 9.4.1, Table 4.9}

C.6.5 Major volcanic eruptions represent a large source of uncertainty for near-term climate projections. While such eruptions are generally not accounted for in climate projections, it is *likely* that they generally result in surface cooling and decreased global-mean land precipitation for up to a few years following the eruption, with climatologically wet regions drying and dry regions wetting (*medium confidence*). {4.4.1, 4.4.4, 8.5.2, Figure 4.19}

[START BOX SPM.3 HERE]

Box SPM.3: Synthesis of regional changes

A new emphasis in the AR6 is climate information relevant to impacts, adaptation, risk assessment and climate service applications that depend on the human or natural system in focus and regional context (see SPMA.3).

This box summarizes and synthesizes the key regional findings on observed, attributed and projected regional changes assessed in the report. It complements SPM Sections B and C to illustrate the regional signature of the current GSAT warming of 1.10°C (0.97°–1.25°C)[11] and how it will evolve in the near and long term under higher warming levels. The methodological basis for the key findings synthesized here is presented in Section SPMA ("From global to regional scales") and the synthesis focuses on changes relevant to the assessment of risks, impacts, adaptation in SPM Section D.5.

Methodology

The criteria that are used to highlight the key findings in each region[12] are based on multiple lines of evidence of changes in climatic impact drivers (CIDs). This includes the assessed observed trends and events and their attribution (where available) and model projections based on global and regional model

[11] For the period 2009–2018 relative to 1850–1900

[12] Focusing on the continental regions defined by WGII and, where relevant, the WGI subcontinental reference regions and also typological regions defined by WGII

ensembles[13]. This Box shows key findings on the direction of change for those CIDs relevant for each region, indicating whether they are assessed as having *high*, *medium* or *low confidence*. Moreover, the combined lines of evidence are used to further highlight those CIDs in a particular region where there is consistency between observed, attributed and projected changes.

Box SPM.3 Table 1 show present day and mid-century findings for RCP8.5 and indicates the regional signature of current warming as well as how this is projected to evolve at future global warming levels[14]. The selection and the regional assessment of the CIDs has been shaped by the interaction with and feedback from the WGII assessment of climate change impacts, adaptation, risk and solutions. (SPM Box.2 Table 1) {TS Table.22}

The intent of SPM.3 Figure 1 is to summarise SPM.3 Table 1, clustering the CIDs into 10 broader groups for each AR6 WGI sub-continental reference region. The figure displays those clusters that include a CID with a consistent message of change across the different lines of assessed evidence or that have a *high confidence* in the projected change. For each region, the Figure shows where there is *medium to high confidence* that change in CIDs has already been experienced and there is *high confidence* will be experienced in the future.

There can be several reasons that result in a disparity of information and/or confidence in one or more lines of evidence in Box SPM.3 Table 1 and Box SPM.3 Figure 1. For example, for several CIDs leading to hazards (such as landslides, avalanches, hail storms, ice storms, tornadoes) the assessment is limited by a lack of long-term homogeneous observations and limitations in process representation in models. In other cases, lack of information is due to an uncertain signal in observations, typically due to a trend that has a smaller magnitude than the natural variability. Also, some regions have relatively fewer published studies, thus limiting the evidence base of documented, attributed or projected CID changes, or the available literature does not agree on the direction of projected change. There are regions for which CIDs show a high confidence projected signal confirmed by observed trend, with attribution studies available, or regions with a high confidence in the projections that lack of one or more other lines of evidence to complement the projections. It is important to note that in such cases, there is no reason to lower the confidence in the projections.{11.9, 12.4, Atlas.5}

The diverse signatures of regional climate change

There is a wide regional diversity in the regional signature of climate change and, from a risk perspective, different regions are *very likely* to experience changes in different combinations of multiple hazards and other CIDs. There are observed and as well as projected changes in multiple CIDs in all regions (*high confidence*), as illustrated in Box SPM.3 Table 1 and Box SPM.3 Figure 1. Some are common to almost all regions (e.g. those related to temperature, relative sea-level rise, ocean acidification) but many are specific to just a few regions (e.g., mean and extreme precipitation change, river flood and drought). (SPMA.3, SPMB, SPMC, SPMD.5) {10.3, 10.4, 10.5, 10.6, 11.9, 12.1, 12.3, 12.4, 12.5, Atlas.5, TS Table.22}

[START BOX SPM.3, TABLE 1 HERE]

Box SPM.3, Table 1: Table of key findings on observed, attributed and projected changes in climatic impact drivers (CIDs) based on TS.22 and TS Appendix 1. Colours indicate the sign of change while

[13] CMIP5, CMIP6 and CORDEX

[14] Box SPM.3 Table 1 builds on the more detailed table TS.22 that summarises projected changes in a range of CIDs with an assessment of the confidence in these from available literature combined with information on observed changes in these indices and attribution studies with the confidence that is associated to their findings. It highlights where these multiple lines of evidence increase the confidence in the observed and projected changes as well as highlighting those regions where changes in CIDs have already been observed and/or attributed. A traceback matrix has been constructed and included in Technical Summary Appendix 1 to document the sources in the underlying chapters of these lines of evidence for each variable and region. It is worth noting that the relevance and quality of evidence coming from the observed trends, attribution studies and projections literature are fundamentally different. Thus the way in which they are combined to generate defensible statements about confidence in the changes involves expert judgement accounting for the variable involved and the region in question.

colour intensity indicates the level of confidence (white=no clear sign of change or low confidence in a change; light=medium confidence; dark=high confidence). Region-by-region information is presented for 28 CIDs for the mid-century time slice and for scenario RCP8.5. The orange frame indicates *very high confidence* in a consistent message of change from observed trends and future projections and attributions studies (with at least one having *high confidence* and both observed and projected changes having at least *medium confidence*). The gray frame indicates *high confidence* of a consistent message of change either from observed and *high confidence* projected changes or from attribution studies and projected changes (of *medium to high confidence.* The yellow frame indicates that there is *medium confidence* of a consistent message of change either from observed and *medium* to *low confidence* projected changes or from attribution studies and projected changes *(of medium to high confidence*). {TS Table 22}

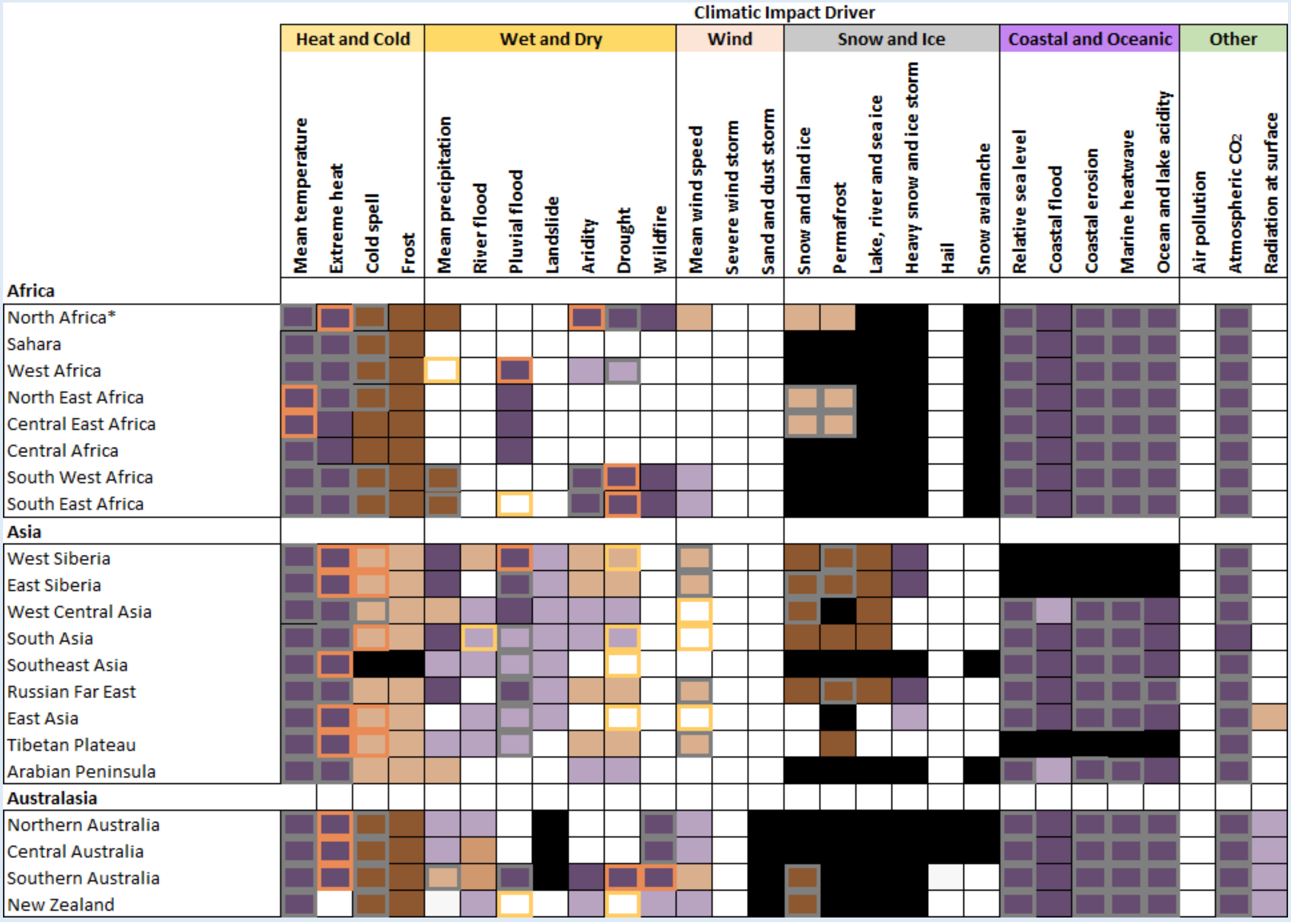

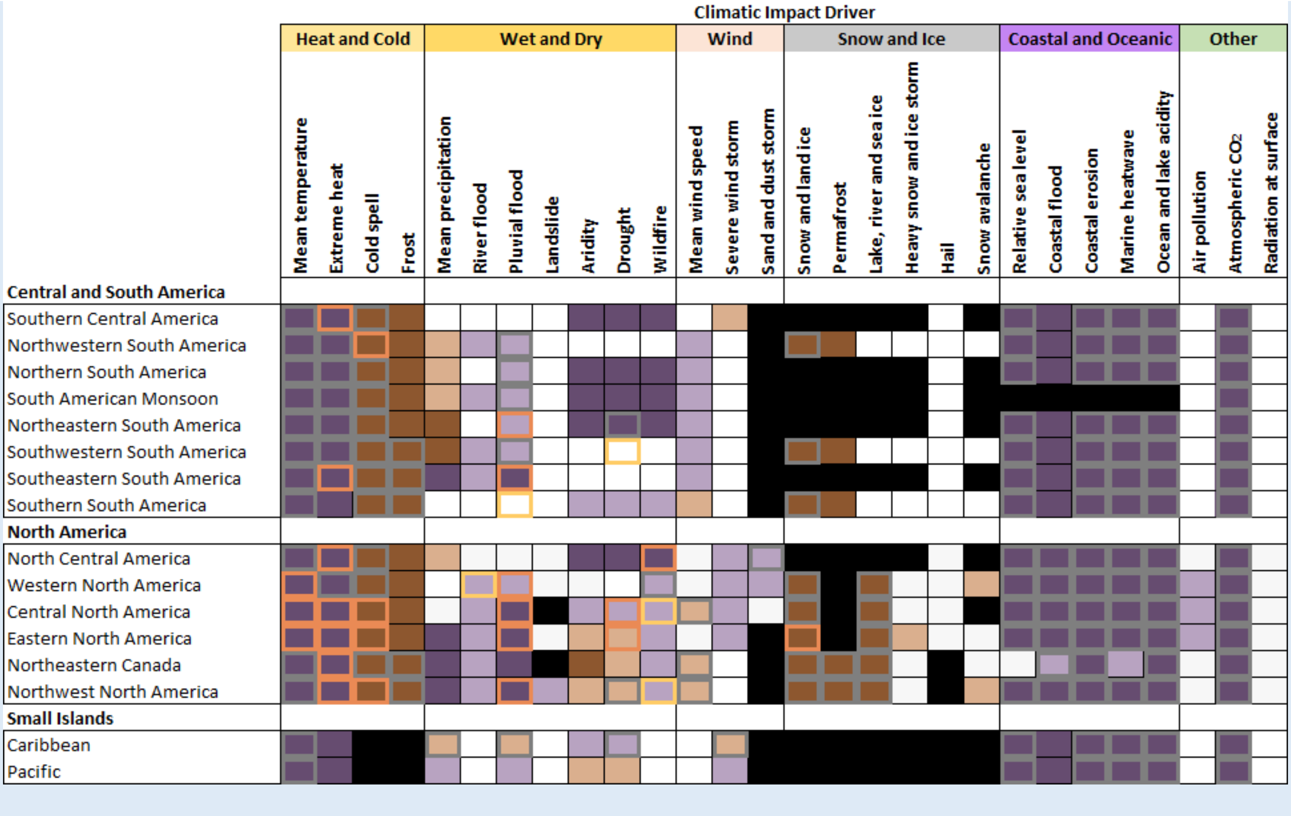
Climatic Impact Driver
Heat and Cold
Wet and Dry
Wind
Snow and Ice
Coastal and Oceanic
Other
Mean temperature
Extreme heat
Cold spell
Frost
Mean precipitation
River flood
Pluvial flood
Landslide
Aridity
Drought
Wildfire
Mean wind speed
Severe wind storm
Sand and dust storm
Snow and land ice
Permafrost
Lake, river and sea ice
Heavy snow and ice storm
Hail
Snow avalanche
Relative sea level
Coastal flood
Coastal erosion
Marine heatwave
Ocean and lake acidity
Air pollution
Atmospheric CO2
Radiation at surface
Central and South America
Southern Central America
Northwestern South America
Northern South America
South American Monsoon
Northeastern South America
Southwestern South America
Southeastern South America
Southern South America
North America
North Central America
Western North America
Central North America
Eastern North America
Northeastern Canada
Northwest North America
Small Islands
Caribbean
Pacific

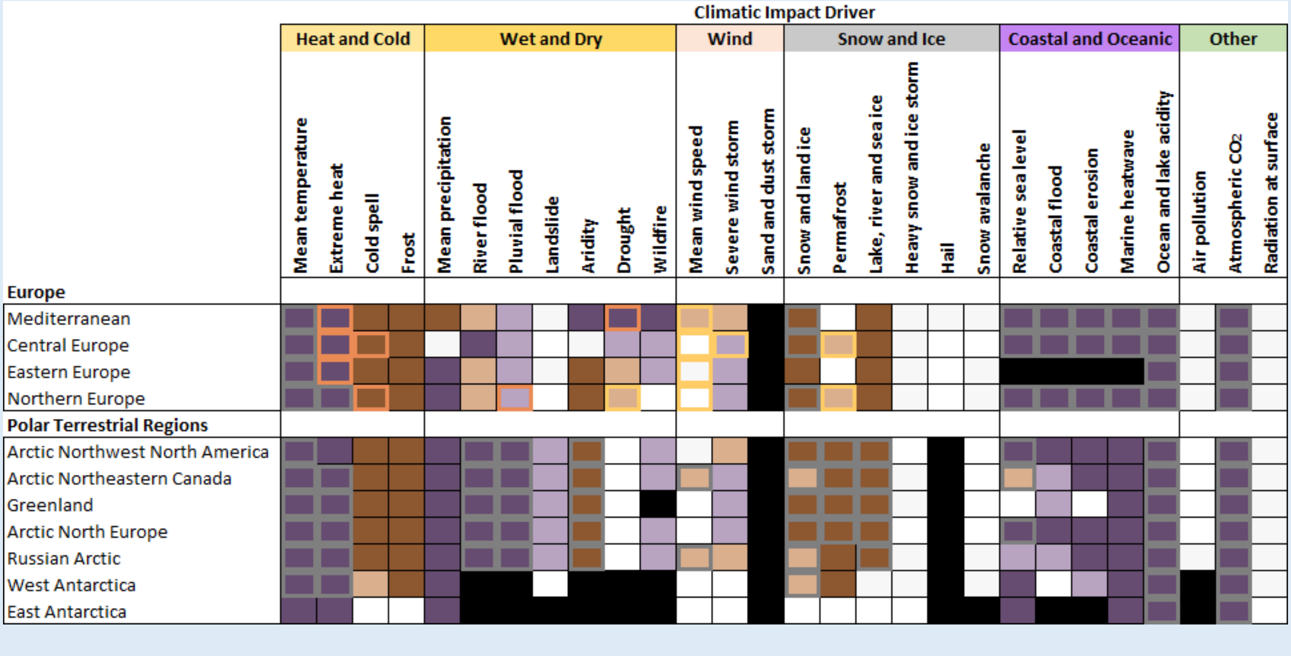
Climatic Impact Driver
Heat and Cold
Wet and Dry
Wind
Snow and Ice
Coastal and Oceanic
Other
Mean temperature
Extreme heat
Cold spell
Frost
Mean precipitation
River flood
Pluvial flood
Landslide
Aridity
Drought
Wildfire
Mean wind speed
Severe wind storm
Sand and dust storm
Snow and land ice
Permafrost
Lake, river and sea ice
Heavy snow and ice storm
Hail
Snow avalanche
Relative sea level
Coastal flood
Coastal erosion
Marine heatwave
Ocean and lake acidity
Air pollution
Atmospheric CO2
Radiation at surface
Europe
Mediterranean
Central Europe
Eastern Europe
Northern Europe
Polar Terrestrial Regions
Arctic Northwest North America
Arctic Northeastern Canada
Greenland
Arctic North Europe
Russian Arctic
West Antarctica
East Antarctica

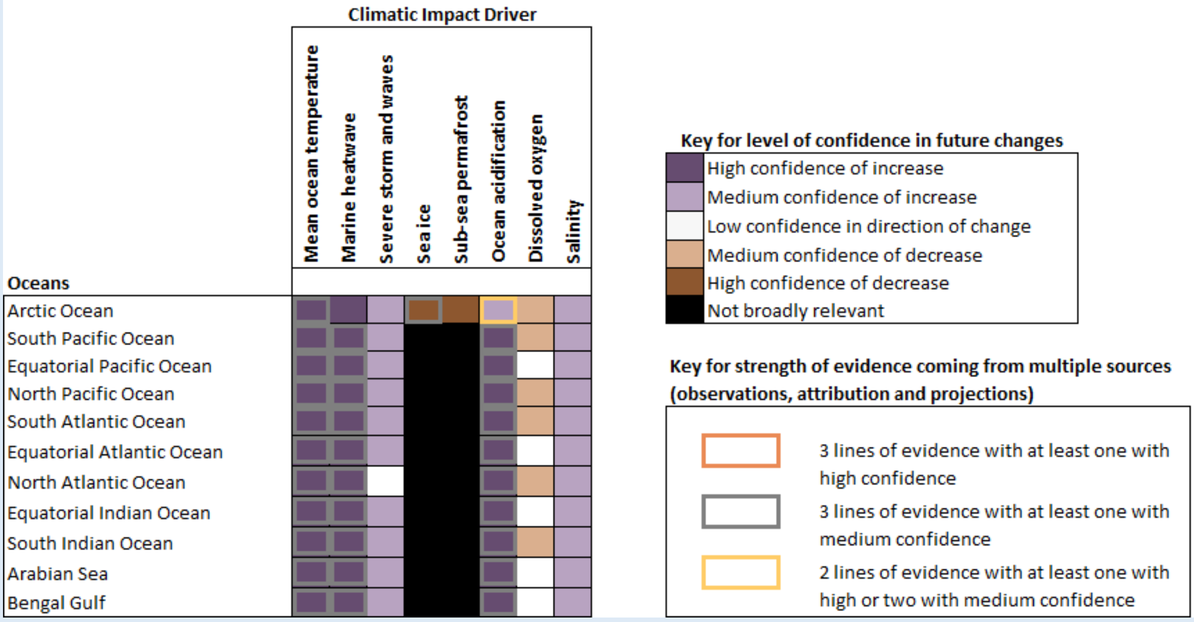

[END BOX SPM.3, TABLE 1 HERE]

[START BOX SPM.3, FIGURE 1 HERE]

Box SPM.3, Figure 1: Synthesis of observed, attributed and projected changes in climatic impact drivers (CIDs) across sub-continental land regions and regional oceanic areas. The original CID categories (upper header of Table 1) are grouped in 10 broader classes each represented with a different colour (colour bar legend). For each region the number of colours in the pie represents the number of classes for which we have high confidence in their direction of change, the +/- sign represents the direction of change and the orange, grey and yellow border represents the additional confidence derived from the multiple lines of evidence (see SPM Box.3 Table 1). {TS.4, TS Table.22}

[END BOX SPM.3, FIGURE 1 HERE]

[END BOX SPM.3 HERE]

D. Climate information to support mitigation and adaptation action

PREAMBLE: *Climate change mitigation and adaptation rely on climate information to support decision making. This section assesses advancements in climate information since AR5 on what would be required from a physical climate point of view to halt global warming and what the effect of implementing specific response measures like carbon-dioxide removal could be. It also assesses how long it would take to observe the effects of climate change mitigation, and how improved understanding of local and regional climate change can support adaptation decisions.*

D.1 Limiting climate change

Limiting further climate change to levels consistent with the Paris Agreement would require substantial and sustained reductions of greenhouse gas emissions. The climate system would continue to warm unless net-zero or net-negative carbon dioxide (CO_2) emissions are reached combined with a stabilization or decrease in net non-CO_2 forcing. Reductions in aerosol precursor emissions to improve air quality would lead to additional net near-term warming, which could be lowered by reducing methane and other ozone precursors simultaneously (*high confidence*). (Figure SPM.10, Table SPM.3) {1.3, Box 1.2, 4.3, 4.7, 5.4, 5.5, 6.5, 6.6, Box 6.2, TS3.4}

D.1.1 Mitigation requirements for stabilizing global warming at specific levels can be quantified using a carbon budget approach that relates cumulative CO_2 emissions to global mean temperature increase. This implies that global anthropogenic CO_2 emissions would at least have to be brought down to net-zero levels to stabilize warming, with the total net amount of anthropogenic CO_2 emissions until that point largely defining the likelihood of keeping warming below a specific temperature limit (*high confidence*). Global temperature can still change by a few tenths of a degree in the decades after net-zero CO_2 emissions are reached (*low confidence*) but estimates of both the sign and precise magnitude of this change remain inconclusive. Reverting global warming to significantly lower temperature levels once it has exceeded a specific temperature limit would require global net CO_2 removal (*high confidence*). (Figure SPM.10, Table SPM.3) {1.3.5, Box 1.2, 4.7.2, 5.5.2, 5.6, TS3.4}

D.1.2 Since AR5, remaining carbon budget estimates have been updated with methodological advances first presented in the IPCC Special Report on Global Warming of 1.5°C (SR1.5), resulting in a significantly improved understanding of their magnitude and larger, yet consistent, estimates (Table SPM.3). Several factors, including estimates of historical warming, future emissions from thawing permafrost, and variations in projected non-CO_2 warming, affect the precise value of remaining carbon budget estimates (*medium confidence*). Compared to SR1.5, the effect of additional Earth system feedbacks has been assessed in more detail but with overall *very low confidence* in the exact magnitude of these contributions. Despite the large uncertainties surrounding the understanding and quantification of the effect of these feedbacks, none of them removes the geophysical requirement that global CO_2 emissions have to at least reach net-zero levels to halt warming. These feedbacks and their uncertainties represent identified additional factors that affect future climate hazards. They scale with each increment in additional globally averaged surface warming and mostly increase the challenge of limiting warming to specific temperature thresholds. (Table SPM.3) {1.3.5, 4.7.2, 5.4, 5.5.2, TS3.4}

[START TABLE SPM.3 HERE]

Table SPM.3: The assessed remaining carbon budget and corresponding uncertainties. Assessed estimates are provided for additional human-induced warming expressed as global average surface air temperature since the recent past (2010–2019). {5.4, 5.5, Figure 5.28, Table 5.8}

Additional warming since 2010-2019 (°C) *(1)	Approx. warming since 1850-1900 (°C) *(1)	Remaining carbon budget *(2) per percentiles of TCRE *(3)		
		33rd ($GtCO_2$)	*50th ($GtCO_2$)*	*67th ($GtCO_2$)*
0.2	1.3	140	90	50
0.3	1.4	320	240	180
0.4	1.5	500	390	310
0.5	1.6	670	540	440
0.6	1.7	850	690	570
0.7	1.8	1030	840	700
0.8	1.9	1210	990	830
0.9	2.0	1390	1140	960
1.0	2.1	1570	1290	1090

Key uncertainties and variations:

- Non-CO_2 scenario variation *(4): ±250 $GtCO_2$
- Non-CO_2 forcing and response uncertainty: -400 to +200 $GtCO_2$ (TBC *(5))
- TCRE distribution uncertainty: +60 to +110 $GtCO_2$ per °C of additional warming
- Historical temperature uncertainty *(1): ±450 $GtCO_2$
- Zero Emissions Commitment (ZEC) *(6): ±410 $GtCO_2$
- Recent emissions uncertainty *(7): ±20 $GtCO_2$ (TBC)

Footnotes:

*(1) Human-induced global surface air temperature increase between 1850-1900 and 2010-2019 has an assessed central estimate of 1.1°C.

*(2) See B1 for assessed historical CO_2 emissions. Assessed Earth system feedbacks like CO_2 released by permafrost thawing are included in the remaining carbon budget estimate in the table at a magnitude of a 135 $GtCO_2$ reduction per °C of additional warming. This estimate of Earth system feedback magnitude is surrounded by a ±100% one standard deviation range.

*(3) TCRE: Transient Climate Response to cumulative CO_2 emissions. Values rounded to nearest 10 $GtCO_2$.

*(4) Variations due to different scenario assumptions related to the future evolution of non-CO_2 emissions in mitigation scenarios reaching net zero CO_2 emissions {SR1.5 Chapter 2}. This contribution will be assessed explicitly in the AR6 Working Group III report.

*(5) Remaining carbon budget variation due to geophysical uncertainty in forcing and temperature response of non-CO_2 emissions. Currently based on SR1.5 and to be updated with final AR6 assessment.

*(6) Estimated for a central TCRE value of 1.6 °C/EgC and a 1-sigma ZEC range of 0.18°C

*(7) Historical emissions uncertainty reflects the uncertainty in historical emissions since 1 January 2015.

[END TABLE SPM.3 HERE]

D.1.3 To limit warming to levels consistent with the Paris Agreement, CO_2 emissions reductions would need to be complemented with reductions of non-CO_2 emissions. Many non-CO_2 emissions are short-lived climate forcers, and the magnitude and sign of their climate influence can vary spatially and temporally. Reductions in aerosols and non-methane ozone precursors to improve air quality would lead to an increase of their warming contribution by 2040, with a *likely* range of 0.1°–0.2°C relative to 2021. It is *unlikely* that methane emissions reductions alone can fully cancel out the near-term warming from reductions in cooling aerosols. However, methane and black carbon (BC) mitigation can contribute towards offsetting the warming associated with sulphur dioxide reductions that accompany the phase-out of CO_2 from specific combustion sources in decarbonisation scenarios (*high confidence*). {6.5.3, 6.6.3, 6.6.4, Box 6.2}

D.1.4 The implementation and efficient enforcement of both the Kigali Amendment to the Montreal Protocol on Substances that Deplete the Ozone Layer and national regulations limiting emissions from hydrofluorocarbons (HFCs) are estimated to lead to a reduction in global warming of less than 0.07°C by 2050 and between 0.2°–0.4°C by 2100, compared to projections where HFC emissions continue unregulated (*medium confidence*). This reduction in warming attributed to HFC regulation results from both substitution of HFCs with alternative lower-warming refrigerants and CO_2 emissions reductions as a result of energy efficiency improvements in refrigeration and air-conditioning equipment. {6.5.3, 6.6.3}

[START FIGURE SPM.10 HERE]

Figure SPM.10: Global mean surface air temperature increase as a function of cumulative total global CO_2 emissions. Assessed observed annual mean GSAT increase since 1850 is shown as a function of assessed historical anthropogenic CO_2 emissions (thin grey line), overlaid with an estimate of the human-induced warming (orange line) and modelled 90% uncertainty range. The grey cone shows the relationship informed by the assessed *likely* TCRE range. Coloured features show the assessed GSAT projections for the core set of five scenarios against their driving cumulative CO_2 emissions. Coloured ranges show the assessed *likely* range while dashed lines show the median. Circle and cross symbols show the location of cumulative CO_2 emissions and assessed median GSAT warming for each of the respective scenarios for the year 2020 (circles) and 2050 (crosses). (SPM Box.2) {Cross-Chapter Box 2.3, 3.3, 4.3.1, 5.2, 5.5, Table 4.1, Table 5.1}

[END FIGURE SPM.10 HERE]

D.2 Geophysical consequences of carbon dioxide removal

Carbon dioxide removal (CDR) methods can sequester CO_2 from the atmosphere (*high confidence*), but the sequestration can be weakened by evolving Earth system feedbacks (*medium confidence*). Wide-ranging potential side-effects of CDR methods have been identified and can either amplify or reduce local climate change and affect the achievement of other societal goals (*high confidence*). These effects are highly project-, region-, and context-specific affecting the level of confidence with which they can be assessed. {4.6, 5.3, 5.6, Figure 5.36, TS Figure.36}

D.2.1 Observations, Earth system understanding, and modelling support the finding that land- and ocean-based CDR methods have the potential to remove CO_2 from the atmosphere (*high confidence*). Similar to when CO_2 is emitted into the atmosphere, Earth system feedbacks would redistribute CO_2 between carbon pools in response to net CDR. Land and ocean sinks would release some CO_2 back into the atmosphere resulting in less CO_2 effectively being removed (*medium confidence*). The effectiveness of CDR, defined as the reduction in atmospheric CO_2 per unit CO_2 sequestered, is largely independent of the magnitude and rate at which CDR is deployed and is greater when CDR is applied in a world with higher atmospheric CO_2 concentrations (*medium confidence*). However, because of a combination of various compensating effects, a given amount of CO_2 removed by CDR results in an approximately constant cooling effect whether removed in a high or a low emission world (*medium confidence*). Reversing the increase in atmospheric CO_2 concentration by CDR will reverse ocean acidification at the sea surface but will not result in rapid amelioration of ocean acidification in the deeper ocean (*medium confidence*). {Figure 5.33, Figure 5.34, 5.3.3, 5.6.2, TS Figure.36}

D.2.2 Both positive and negative potential side-effects of the deployment of CDR measures have been identified, and Earth system feedbacks that decrease carbon uptake on land and in the ocean or change local and regional climate can in turn limit the CO_2 sequestration potential of specific CDR measures (*medium confidence*). Identified side-effects can be biogeochemical (e.g., changes in non-CO_2 emissions), biophysical (e.g., changes in hydrology or surface reflectivity) (*high confidence*), or related to other societal issues like water availability, food security and biodiversity[15] (*high confidence*). The direction and magnitude of the side-effects of individual CDR methods vary, are often project- and region-specific and are associated with widely varying levels of confidence. The effects of terminating CDR are expected to be small for the deployment of CDR that is applied at scales currently deemed possible (*medium confidence*). {Figure 5.36, 5.6.2, 4.6.3}

D.3 Geophysical consequences of solar radiation modification

Masking global greenhouse gas warming through solar radiation modification (SRM) would *likely* be incomplete, and large residual regional and seasonal climate changes would remain (*high confidence*). Detailed understanding of the climate response to SRM remains subject to large uncertainties. {4.6, 5.6, 8.5, 8.6}

D.3.1 Solar radiation modification (SRM) would act to mask, but not undo, greenhouse gas-induced warming. The cancellation of warming by SRM would *likely* be incomplete, and large residual regional and seasonal climate changes would remain (*high confidence*). It is *very likely* that sudden implementation or termination of SRM could drive sudden changes in the water cycle both globally and regionally. SRM deployment could reduce plant and soil respiration as well as temper the effects of warming on ocean carbon uptake, and would thus *likely* increase global land and ocean sinks (*medium confidence*). SRM would not counteract ocean acidification (*high confidence*). {4.6.3, 5.6.3, 8.5.3, 8.6.2, 8.6.3}

D.3.2 Despite progress since AR5 in understanding the climate effects of and responses of biogeochemical and water cycles to SRM, understanding of important climate processes associated with specific SRM approaches and the interactions between these processes still suffer from large uncertainties (*high confidence*). There is *high confidence*, as assessed in AR5, that a sudden and sustained termination of SRM would cause a rapid increase in global warming, but a gradual phase-out of SRM combined with mitigation and deploying global scale net CDR would *likely* avoid these large rates of warming. {4.6.3, 5.6.3, 8.5.3, 8.6.2, 8.6.3}

D.4 Detecting the effect of emissions reductions

Reductions in greenhouse gas emissions would limit globally averaged surface warming, but the resulting slowdown in warming would be temporarily masked by natural year-to-year variability (*high confidence*), as well as by additional warming due to reductions of cooling aerosols – even when accompanied by reductions in other short-lived climate forcers. The detection time of mitigation benefits for surface air temperature would therefore be about 25–30 years for the global mean and near the end of the century at regional scales (*medium confidence*). (Box SPM.2) {4.4, 4.6, 6.6}

D.4.1 The extent to which natural variability will mask the effect of mitigation on globally averaged surface warming will depend on the magnitude of greenhouse gas emissions reductions. The effect of emissions reductions on the globally averaged warming rate in surface air temperature would not be reliably detectable in the near term (2021–2040) (*high confidence*). Even for pathways with rapid decreases to net-zero and negative CO_2 emissions consistent with keeping warming to 1.5°C or 2°C,

[15] An assessment of the socio-economic and governance dimensions of CDR deployment, including its potential side-effects, is carried out by Working Group III.

trends in surface air temperature would only be detected after 25–30 years globally and near the end of the century at regional scales (*medium confidence*). (Box SPM.2) {4.6.3}

D.4.2 The effect of emissions reductions would first be detectable in changing atmospheric concentrations of climate forcers (*high confidence*). Time scales over which these changes can be detected differ between CO_2 and short-lived climate forcers. Changes in concentrations of long-lived forcers like CO_2 could be detected in about ten to fifteen years (*high confidence*). In contrast, concentrations of short-lived climate forcers, like aerosols and ozone, respond to emission reductions within days or months, and most strongly near areas where emissions of these compounds are reduced. Changes in their concentrations can therefore be detected in less than a year (*high confidence).* (Box SPM.2) {6.5.1, 6.5.2, 6.6.3}

D.4.3 CO_2 and methane emissions cause an important contribution to global warming on time scales of a decade or two (*high confidence*). Across the core set of scenarios assessed in AR6, which spans a wide but not the full range of climate mitigation and air pollution control options, changes in emissions of short-lived climate forcers, including methane, will *very likely* cause a relative warming in globally averaged surface temperature from 2020 to 2040, with a *likely* range of 0°C to 0.3°C. Because the effect of short-lived climate forcers decays rapidly – within days to decades after emission – the net long-term global temperature effect from all anthropogenic emissions is predominantly determined by CO_2. (Box SPM.2) {6.5.1, 6.5.2, 6.6.3}

D.5 Climate information and societal linkages

Useful climate information for vulnerability, impacts, adaptation, and climate service applications depends on the regional context and sectoral assets in focus. Irrespective of the emission pathway that is followed, multiple climatic impact drivers will continue to change over all regions over the next decades as well as the longer course of the century (*high confidence*). Strong climate change mitigation and air quality measures would lead to notable air quality improvements (*high confidence*). Improved understanding of user needs and co-designing of climate information can enhance the provision of scientific evidence for decision making (*high confidence*). (Box SPM.2, Box SPM.3) {6.2, 6.4, 6.5, 6.5, 6.6, 10.5, 10.6, 11.2, 11.8, 12.1, 12.2, 12.4, 12.5, 12.6, Atlas1.1, Atlas1.2, TS Tables.2-10}

D.5.1 Information about climatic impact drivers and their changes by global warming levels provide the hazard context for evaluating impacts and risk at regional and sectoral levels, and can support syntheses of key risks and aggregation into IPCC Reasons For Concern. Many hazard characteristics have a direct relation to the level of global warming (*medium confidence*), while other drivers also heavily depend on the time dimension or the scenario that is followed (*medium confidence*), while tipping points cannot be excluded (*medium confidence*). (Box SPM.3) {11.2.4, 11.2.6, Box 11.4, 12.5.2}

D.5.2 There is *high confidence* that several climatic impact drivers (surface air temperature, sea surface temperature, sea level rise relative to local coasts, and ocean acidification) will continue to change in all regions of the world over the 21st century irrespective of the emission scenario. A broader range of climatic impact drivers (such as drought or extreme rainfall) have regionally specific changes (*high confidence*). Warming trends would increase the likelihood that different hazards (such as drought) would occur on top of already extreme heat conditions, which would lead to compounding effects (*high confidence*). (Box SPM.2, Box SPM.3) {11.8, 12.2, 12.3, 12.4, 12.5.2, TS Tables.2-10}

D.5.3 Projections of global and local air quality are predominantly driven by changes in precursor emissions rather than climate (*high confidence*). Strong climate change mitigation and air quality measures would lead to substantial reductions in global surface air pollution (for ozone and particulate matter) while weak climate and air pollution mitigation would lead to strong increases in the concentrations of these air pollutants throughout the whole century (*high confidence*). Rapid decarbonisation strategies lead to air quality improvements but would not be sufficient to achieve, in the near term, air quality guideline values set by the World Health Organization in some highly polluted regions (*high confidence*). {6.2.1, 6.4, 6.5, 6.6, TS3.5, TS Figure.32}

D.5.4 It is *virtually certain* that complex climate change information is understood differently by different groups of people. Since AR5, there has been considerable progress in understanding climate information user needs, better facilitation of user engagement, further translation of climate data into impacts- and risk-relevant indices, and an appreciation of climate scientists to involve communication specialists and social scientists to support the co-design and co-development process that is fundamental to a successful climate service. Climate services are being developed across regions, sectors (e.g., agriculture, water, energy, health), timescales (from sub-seasonal to multi-decadal) and target users (*high confidence*). User needs and decision-making contexts are very diverse and there is no 'one size fits all' solution to climate services (*very high confidence*). Processes that support collaborative learning and knowledge production involving a diversity of expertise, including both climate scientists and decision makers, can facilitate the integration of science evidence into decision making (*high confidence*). {10.5, 12.3, 12.6, TS4.1, TS Figure.7, TS Figure.33}

Figures

[START FIGURE SPM.1 HERE]

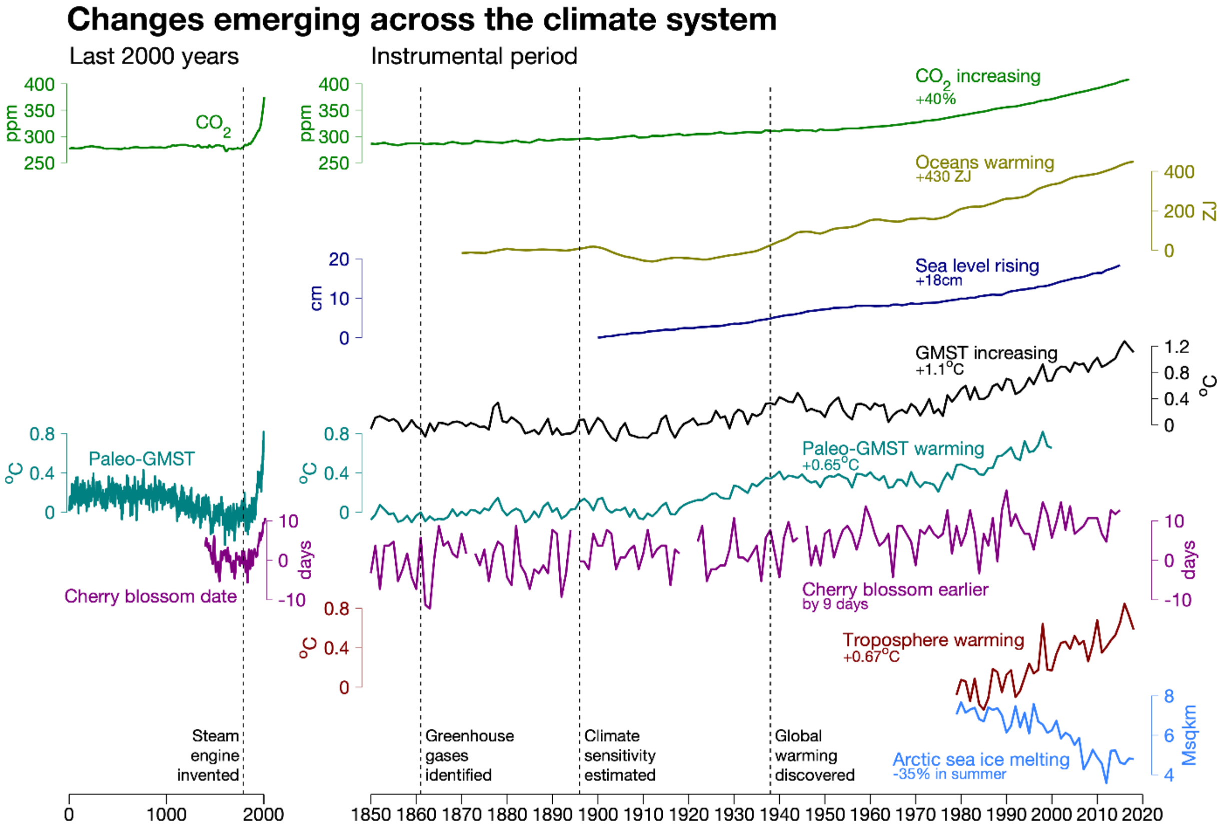

The intent of this figure is to highlight that multiple climate indicators show that changes are emerging across the climate system, from the atmosphere to the ocean to the cryosphere and biosphere. This emergence is seen over the instrumental record (1850-2018) and over the last 2000 years.

Figure SPM.1: Indicators (from top to bottom): atmospheric carbon dioxide concentration, ocean heat content, global sea level, GMST from HadCRUT5, GMST from PAGES2k, Kyoto cherry blossom date, global lower tropospheric temperature from RSS, Arctic September sea ice extent. Key moments in the history of climate science are indicated: the invention of the efficient steam engine by James Watt in 1790, the identification of the primary greenhouse gases by John Tyndall in 1861, the first estimate of climate sensitivity by Svante Arrhenius in 1896, and the discovery that the world was warming by Guy Callendar in 1938.Quantitatively, the CO_2 concentration increased by 40% over 1850-2018, the ocean heat content increase since 1860 is equal to 430ZJ and the global sea level rose by 18cm since 1900. The GMST increased by 1.1°C over 1850-2018 while the warming estimated from paleo GMST is equal to 0.65°C over 1850-2000 and the troposphere warmed by 0.67°C during the satellite era. Sea ice declined in the Arctic in summer by 35% since 1979.

[END FIGURE SPM.1 HERE]

[START FIGURE SPM.2 HERE]

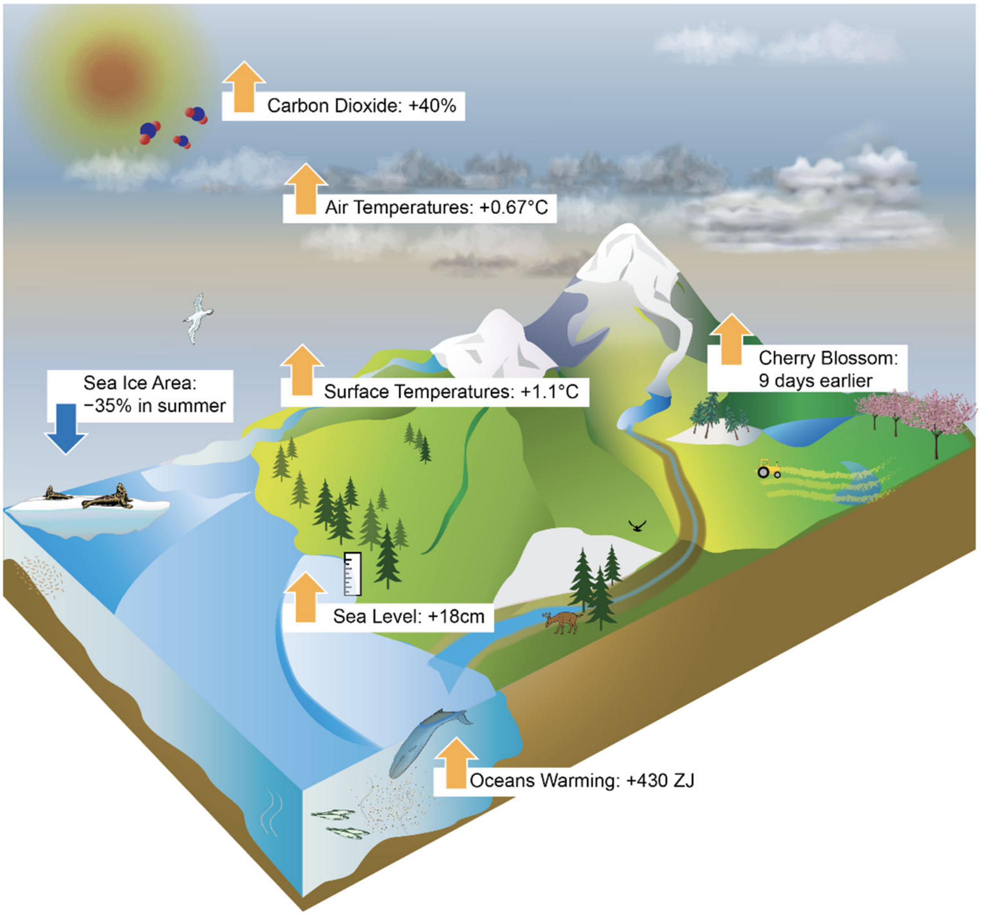

Figure SPM.2: Indicators of change across all components of the Earth System as denoted in Figure SPM.1 including the observed magnitudes over the periods included therein. [Placeholder: This figure will be developed to include uncertainty ranges and associated confidences. Please consider SROCC Figure TS.2 of FAQ2.2 Figure 1 as a basis for development for this figure.]

[END FIGURE SPM.2 HERE]

[START FIGURE SPM.3 HERE]

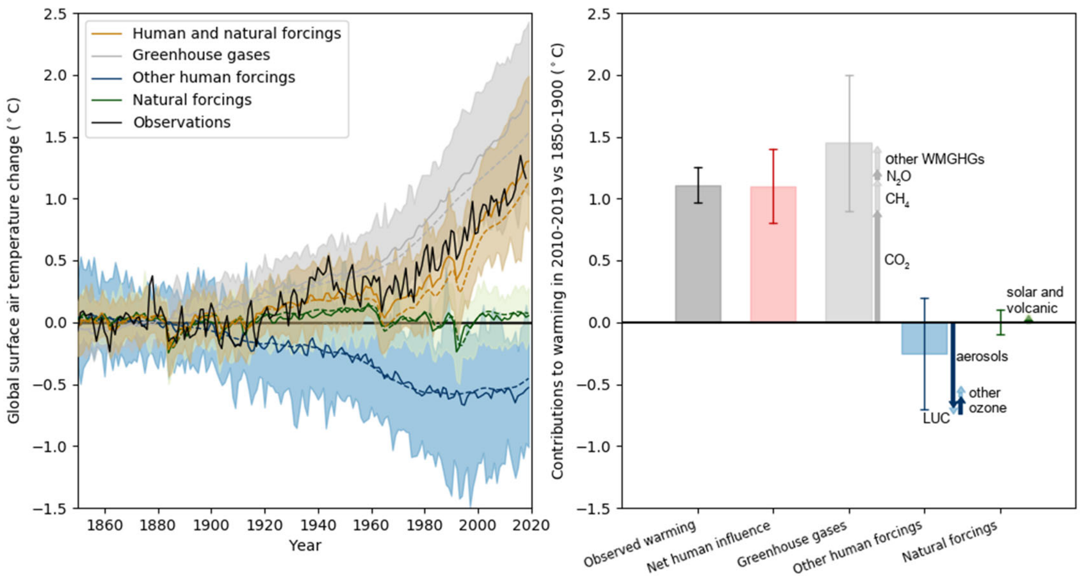

This figure shows the contributions of different forcing agents to observed global surface temperature changes.

Figure SPM.3: Left panel shows global surface air temperature (GSAT) in observations (black), simulations with human and natural forcings (orange), well-mixed greenhouse gases only (grey), aerosols and other human forcings (blue), and natural forcings only (green) in CMIP6 models (solid lines show the mean and shading shows the 5-95% range) and in an emulator (dashed lines show the median). Right panel compares the observed warming in 2010-2019 relative to 1850-1900 with the assessed *likely* ranges attributable to net human influence (red), well-mixed greenhouse gases (grey), other human forcings (blue), and natural forcings (green). Shaded bars show the mid-points of the assessed ranges. Grey arrows show the median warming contributions from individual greenhouse gases, derived based on assessed ERF changes and an emulator. Similarly blue arrows show the contributions from other anthropogenic forcings, where the arrow labelled 'other' represents the net effects of black carbon on snow, contrails and stratospheric water vapour, the arrow labelled 'LUC' represents the physical effects of land-use change, and the green arrow represents the net effects of solar and volcanic forcing. Note that the sums of the individual forcing contributions based on the emulator do not agree exactly with the centre of the assessed ranges for each group of forcings, which draw on multiple lines of evidence, but they are consistent to within the uncertainties. {Figure TS.13}

[END FIGURE SPM.3 HERE]

[START FIGURE SPM.4 HERE]

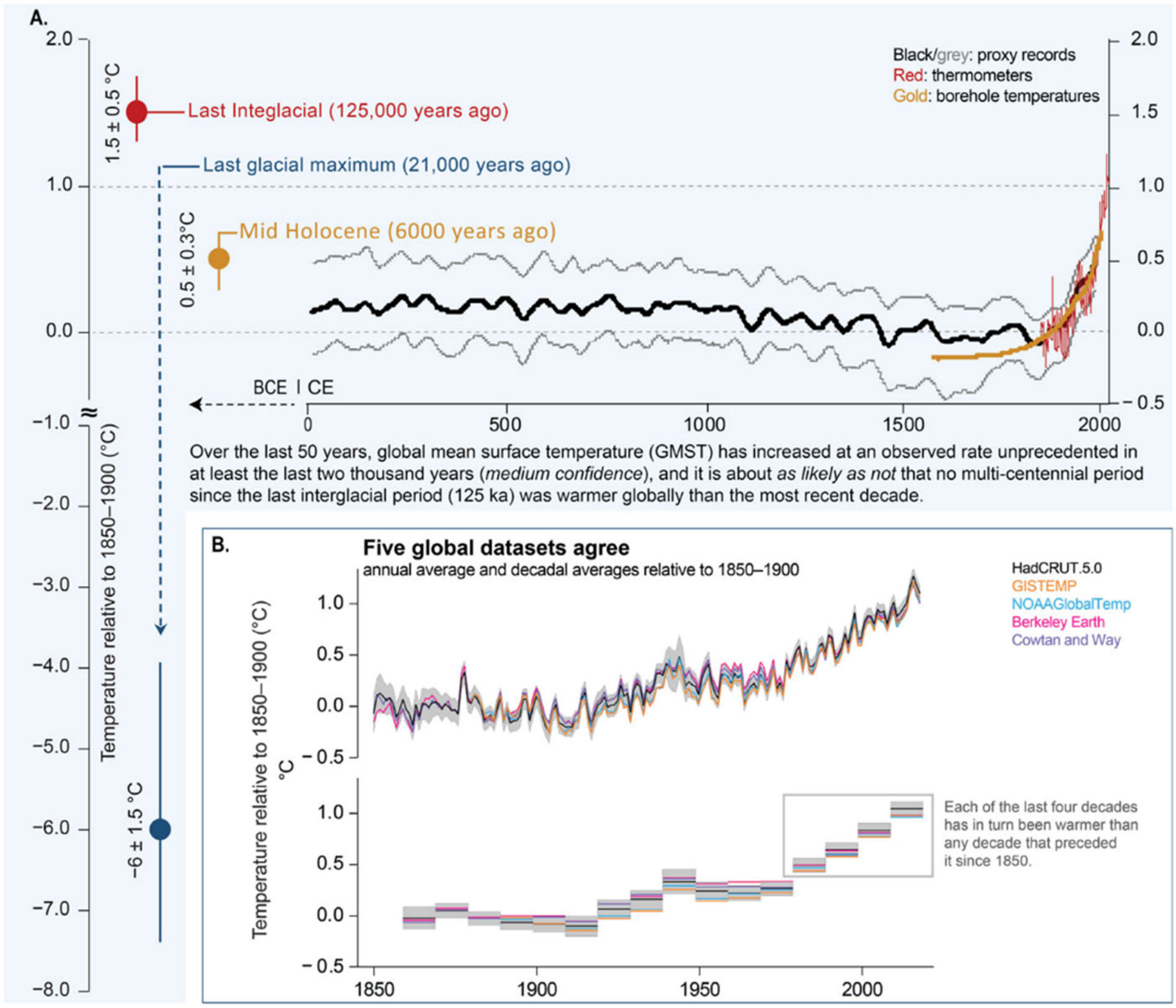

The purpose of this figure shows how global temperatures have changed since 1850 and in a longer-term context.

Figure SPM.4: (a) Global mean surface temperature during the past 2000 years (median multi-method reconstruction (black line), with 2.5th and 97.5th percentiles of the ensemble members (grey bands). The mean global ground surface temperature reconstructed from borehole temperature profiles (gold line), and the average of three instrumental-based datasets extending to 1850 (red line) are also shown for comparison. Large circles along left edge are best estimates for global mean temperature (bars are ± 2 SD) for mid-Holocene (around 6000 years ago), last glacial maximum (around 20,000 years ago), and last interglacial period (around 125,000 years ago). (b) Combined land and sea surface temperatures based on five different datasets. Top panel: annually resolved temperatures. Bottom panel: decadal mean values. Grey shading in both panels shows the uncertainty associated with one of the datasets (HadCRUTv5). All temperatures are anomalies relative to the 1850-1900 reference period. {2.3.1, TS.12}

[END FIGURE SPM.4 HERE]

[START FIGURE SPM.5 HERE]

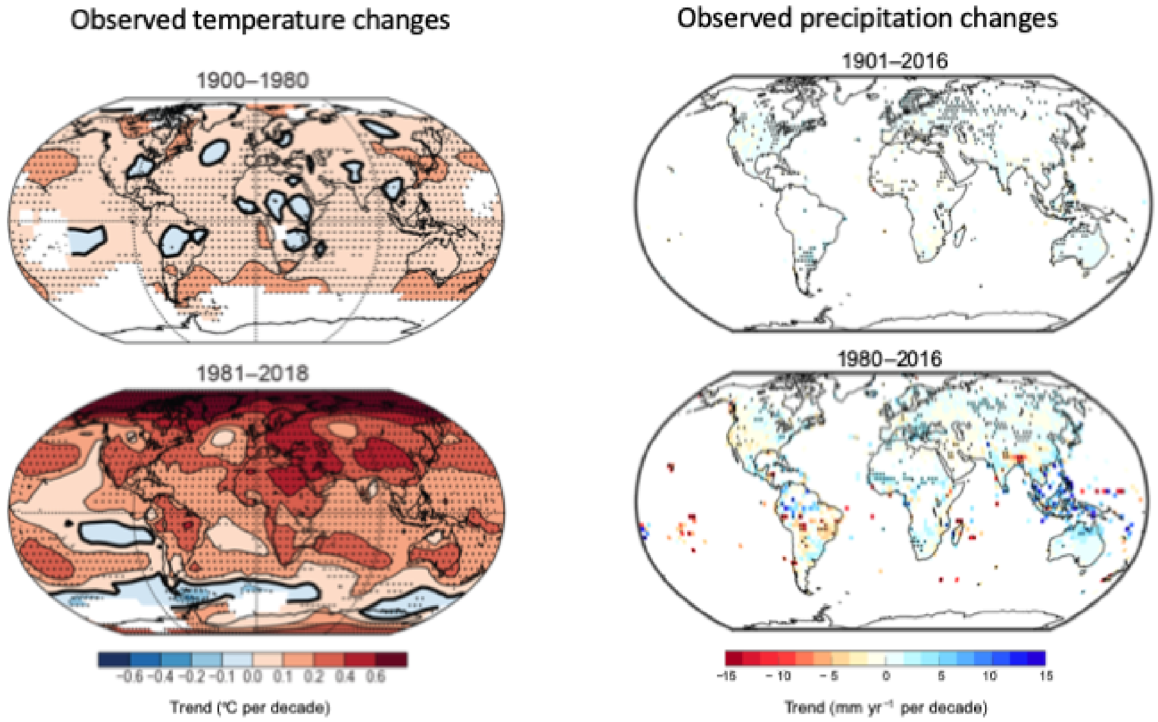

Figure SPM.5: Trends in surface temperatures from HadCRUTv5 (left panels) and precipitation from GPCCv8 (right panels) with statistical significance denoted by crosses. Top panels denote trends over the early 20th century [note that in FGD it is proposed to cut the GPCC series analysis to 1980] and bottom panels denote trends over the more recent 40 years. Data are only shown where sufficient data exists over the entire time span of each panel. {Figure 2.11, Figure 2.14, TS.12, TS.19}

[START FIGURE SPM.5 HERE]

[START FIGURE SPM.6 HERE]

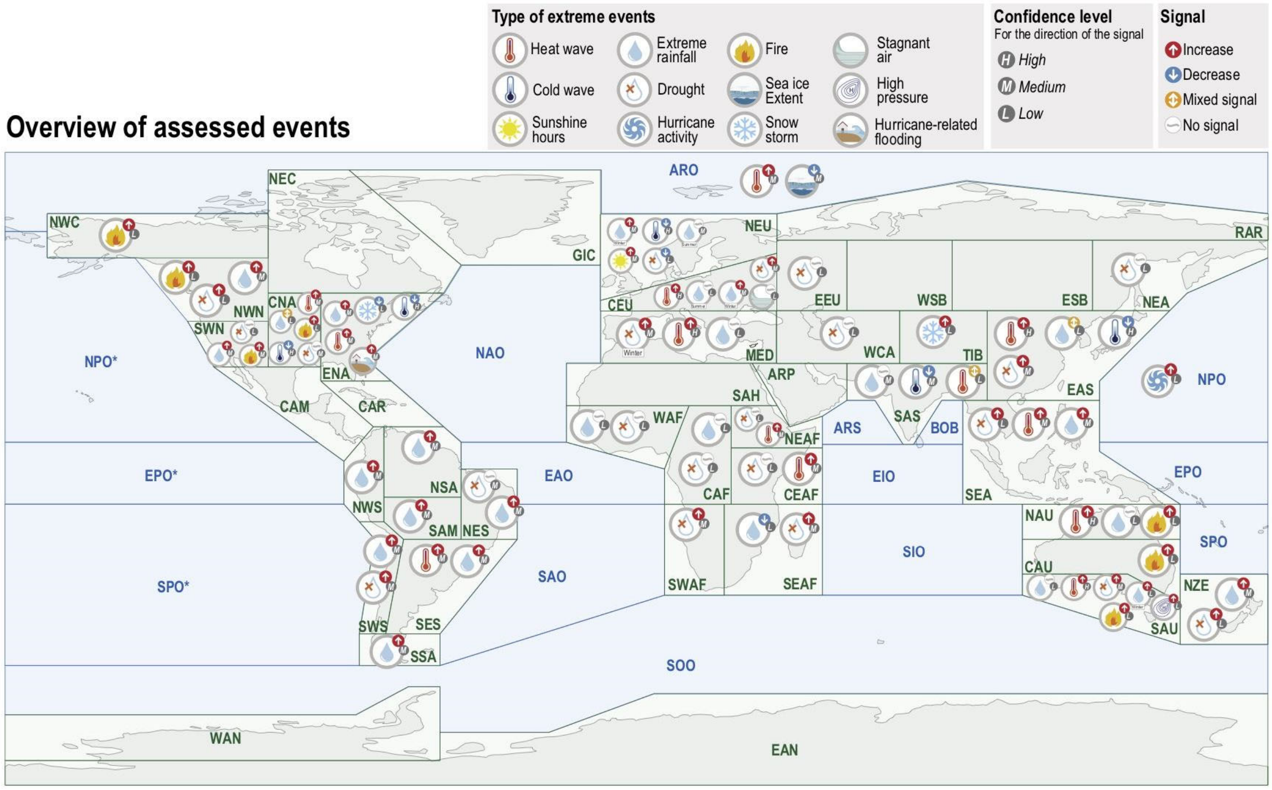

The purpose of this figure is to show that we now have a lot of evidence that is attributed to anthropogenic climate change in different regions of the world for many different types of extreme events

Figure SPM.6: The symbols depict types of extreme events for which one or more such events have been studied in the event attribution framework (see Appendix Table 11.A.1). The location of symbols does not indicate the places of the event occurrence as the symbols represent the synthesized assessment of all studies for the same type of events occurring in the region. The arrows indicate the direction of changes in the intensity and likelihood of the events due to anthropogenic climate change. A "mixed signal" indicates that different studies found different results regarding the direction of changes in magnitude and frequency, depending on the definition of the event {11.2.5, Appendix Table 11.A.1, TS Cross-Section Box 2 Figure 2, Box TS.5 Figure 2}

[END FIGURE SPM.6 HERE]

[START BOX SPM.2, FIGURE 1 HERE]

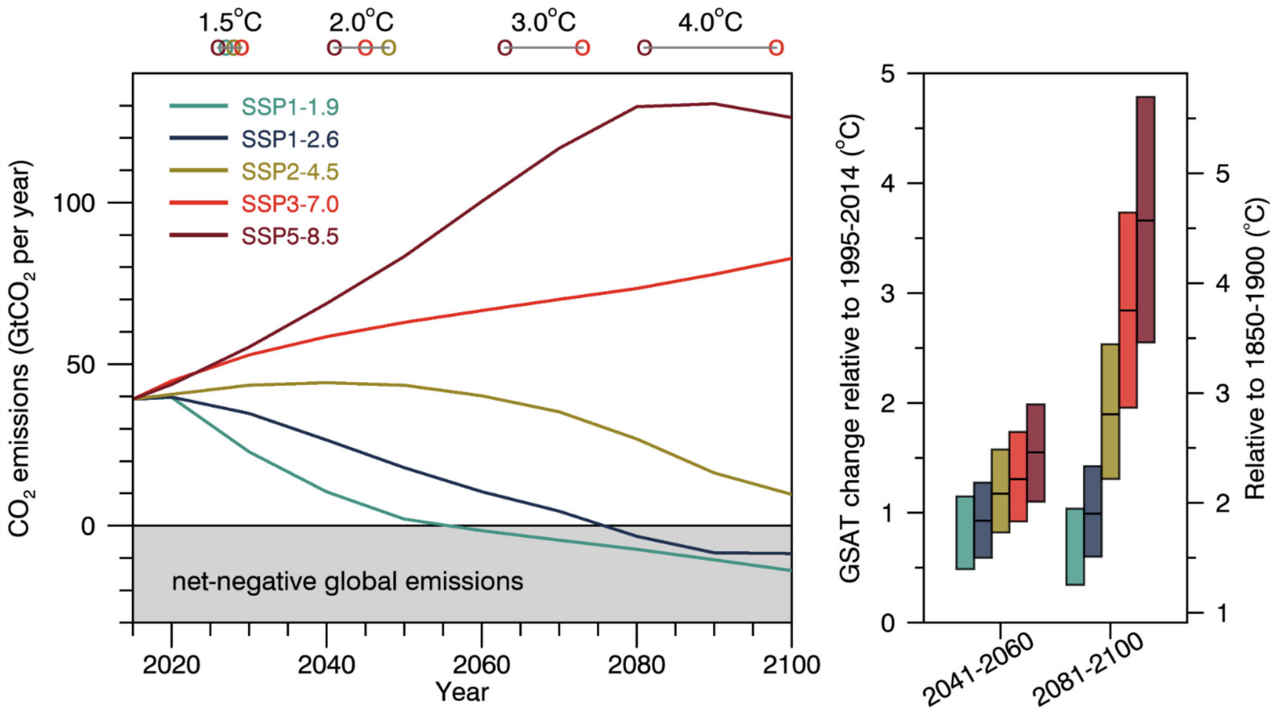

The purpose of this figure is to connect scenarios, scenario-based projections and warming levels. The figure synthesizes the dimensions of integration by providing a visual link between SSPs, annual CO_2 emissions, the assessed GSAT ranges for SSP scenarios for the end of the 21st century and the time periods at which the specific warming levels are reached.

Box SPM.2, Figure 1: Combining ranges of projected temperature change and the time when particular warming levels are reached: time series of SSP-based annual CO_2 emissions from fossil fuel combustion and land use change for the core set of five illustrative SSP scenarios used in this report. SSP-based temperature projections for two time periods in the 21st century (vertical bars to the right of the panel). Note that the projected changes in GSAT are not based on raw model outputs, but on multiple and converging lines of evidence that enable the narrowing of the range of possible temperature outcomes. Adding 0.91°C to the best estimate and the ranges for the selected time periods provides an approximation to the 1850-1900 baseline (see Box TS.4, Table 1). Time when particular warming levels relative to 1850-1900 are reached in the SSPs (along the top axis, with circles under each warming level indicating best estimates for the individual scenarios. 5-95% uncertainty ranges will be added in FGD version). {1.6.1, 1.6.3, 4.3.4, 5.5.2, TS Cross-Section Boxes 1 and 2}

[END BOX SPM.2, FIGURE 1 HERE]

[START FIGURE SPM.7 HERE]

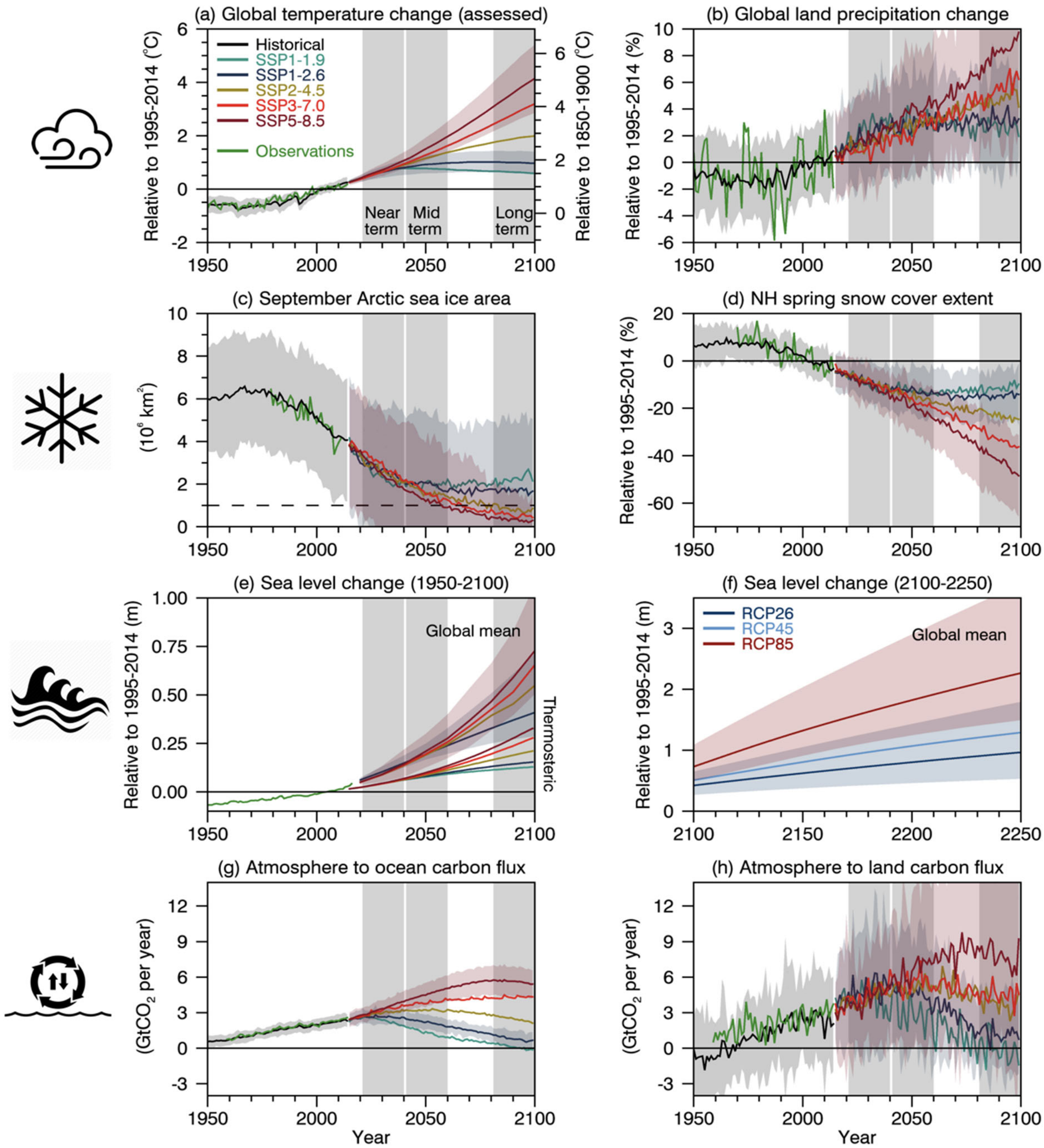

The figure highlights the models' ability to capture recent trends in key climate change indicators, the different climate futures associated with different emissions scenarios (thick lines), the uncertainties due to both intermodel spread and internal climate variability for a given emission scenario (shading), the irreversibility of the global mean sea level rise at the multi-century timescale, and the non-linear response of the carbon cycle to global warming.

Figure SPM.7: Observed and projected time series of changes in (a) Annual global mean near-surface air temperature (GSAT), (b) Annual global land precipitation, (c) September Arctic sea ice area, (d) Northern Hemisphere (NH) spring snow cover extent, (e) Annual sea level change (global mean and thermosteric contribution from warming alone), (f) Annual Global sea level beyond 2100 (note that the axes differ to those in (e), (f) Annual ocean carbon sink, (g) Annual land carbon sink. Note that projected changes in GSAT are not based on raw model outputs, but on multiple and converging lines of evidence that enable to narrow the range of possible temperature outcomes. Near-term, mid-term and long-term climate changes as defined in the AR6 are bounded by grey bars. {TS Cross-Section Box 1, Figure 1}

[END FIGURE SPM.7 HERE]

[START FIGURE SPM.8 HERE]

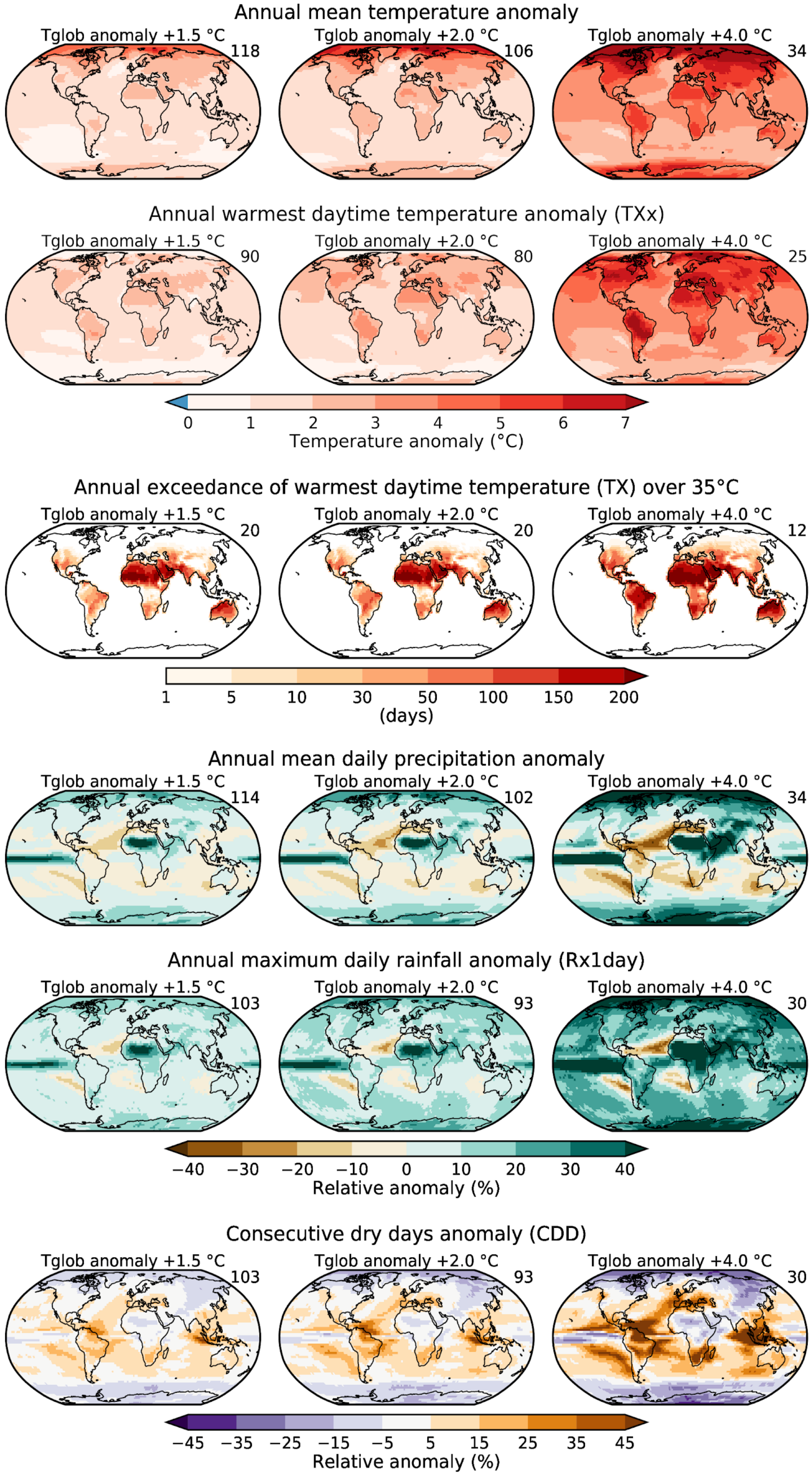

The purpose of the figure is to show the regional distribution of changes across a range of indicators, as a function of warming level. It highlights that even small changes in global warming lead to large changes in extremes.

Figure SPM.8: Global maps of projected changes at increasing global warming levels above preindustrial level in (from top to bottom) annual mean temperature, daytime temperature of annual warmest day, annual exceedance of bias-adjusted (using quantile delta mapping) warmest daytime temperature (TX) over 35°C, annual mean precipitation, annual maximum daily precipitation, and annual maximum of consecutive dry days for 1.5°C (left), 2°C (middle) and 4°C (right) global surface air temperature above 1850-1900. {TS Cross-Section Box 2 Figure 1}

[END FIGURE SPM.8 HERE]

[START FIGURE SPM.9 HERE]

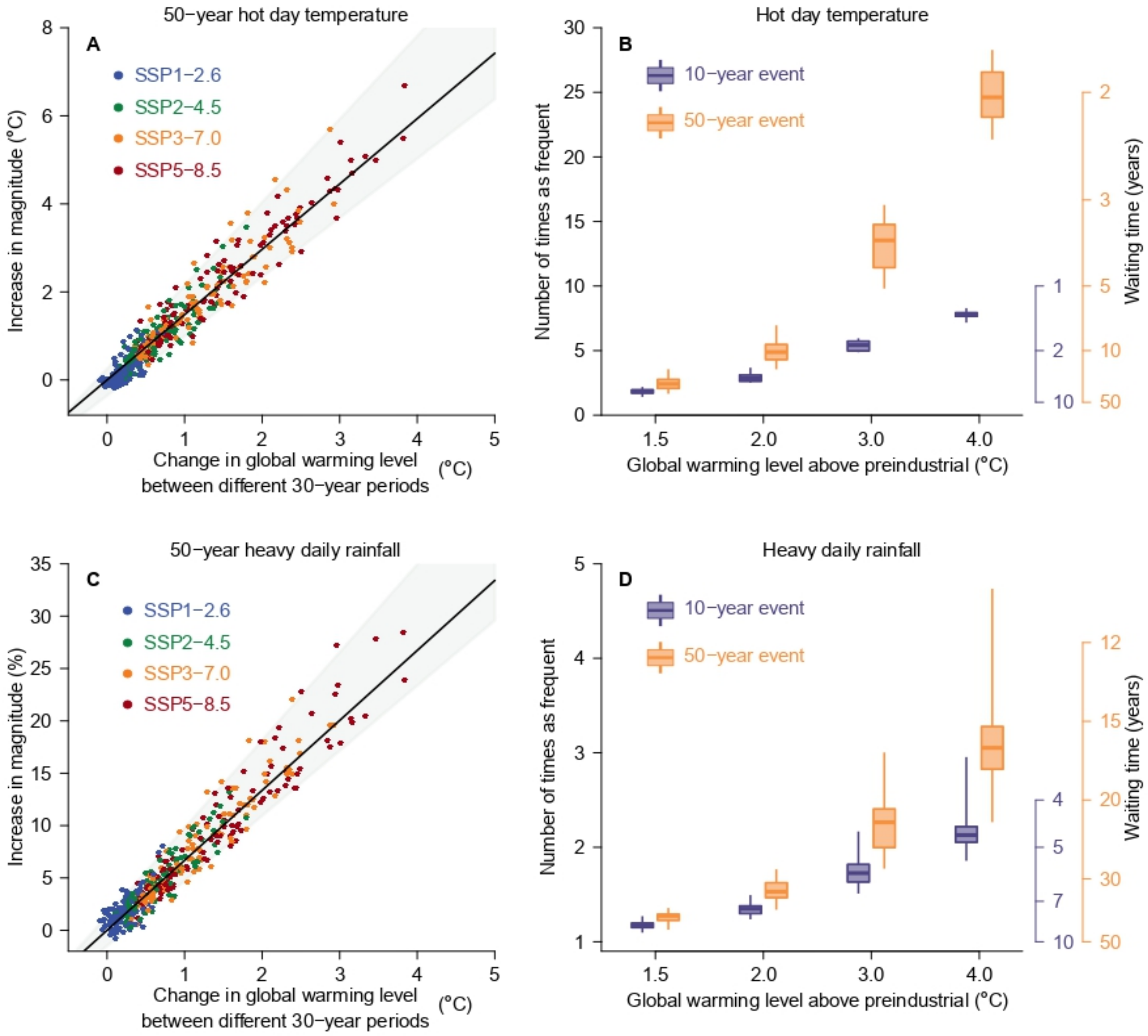

Figure SPM.9: Projected changes in the magnitude and frequency of extreme temperature and precipitation under different global warming levels. A, C: Global land median changes in the 50-year return values of annual maximum daily maximum temperature (A) and annual maximum one-day precipitation (C) with respect to global warming level in the CMIP6 multi-model ensemble simulations under different future forcing scenarios. The black solid lines mark the median regression lines of the scatter points, while the grey envelopes bound the 5-95% regression lines of the scatter points. B, D: Global land median changes in the frequencies of hottest day temperature (B) and heaviest day rainfall amount (D) that occurs once in 10 year (10-year event) or once in 50 years (50-year event) on average in the 1°C warming climate under different warming levels. The average waiting time for such events to occur is marked on the right side of the plots. The horizontal line and the height of the box represent median and interquartile range of the changes and the whiskers extend to the full range of the change estimated from simulations by different CMIP6 models under different SSP scenarios. Warming level is defined as global mean near surface air temperature relative to 1850-1990 mean. The figure highlights that: 1) the projected changes in the magnitude of extreme temperature and extreme precipitation increase with global warming level near-linearly, independent of SSP scenarios; 2) projected changes in the frequency increases with global warming level non-linearly; 3) increase in the frequency is larger for less frequent events. [Placeholder: The figure is based on one run per model from all models participating in CMIP6 whose relevant simulations were available at the time of analysis, which will be re-computed for FGD with large-ensemble model runs of CMIP6 models to obtained more robust estimate]

[END FIGURE SPM.9 HERE]

[START BOX SPM.3, FIGURE 1 HERE]

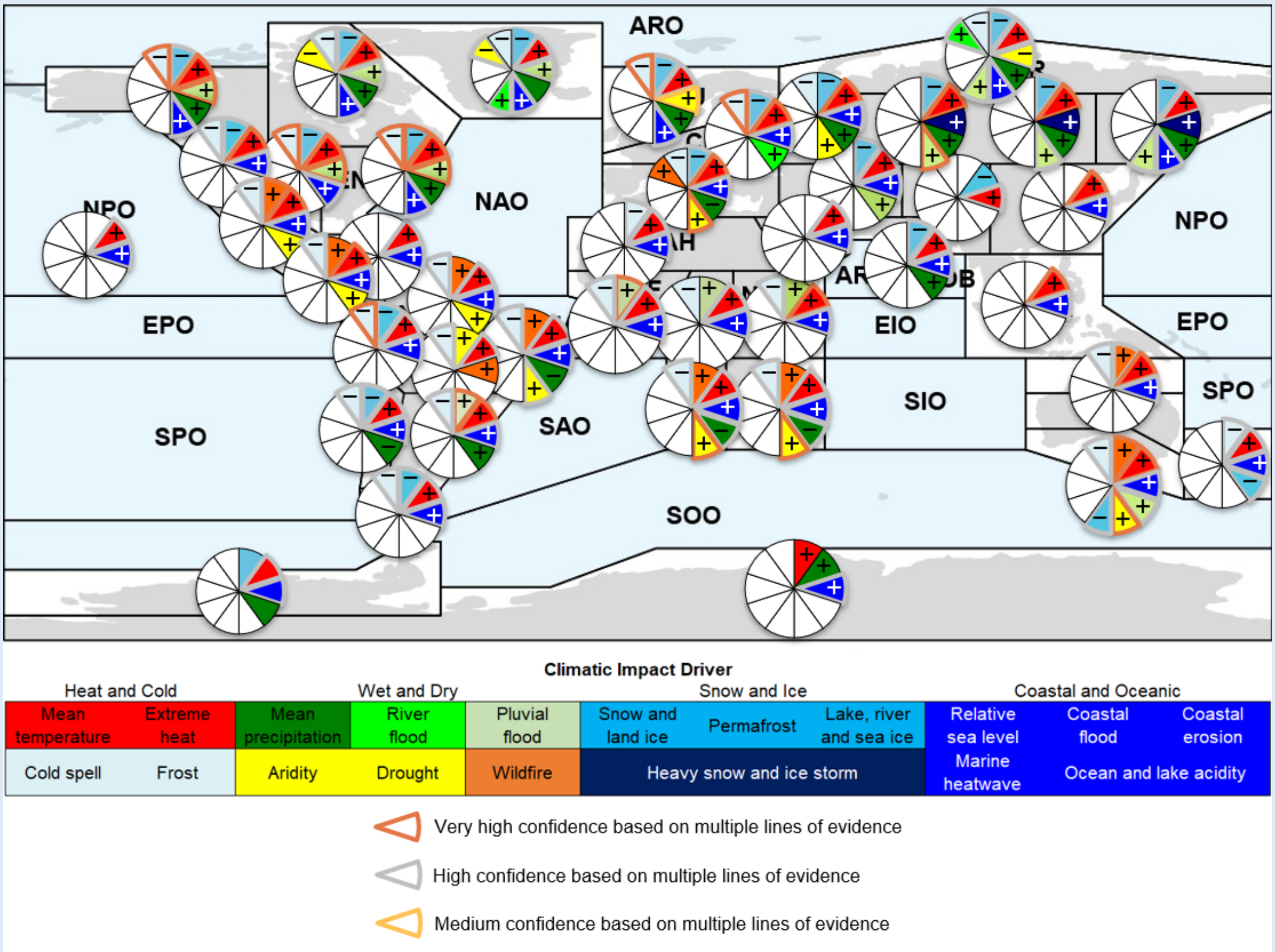

Box SPM.3, Figure 1: Synthesis of observed, attributed and projected changes in climatic impact drivers (CIDs) across sub-continental land regions and regional oceanic areas. The original CID categories (upper header of Table 1) are grouped in 10 broader classes each represented with a different colour (colour bar legend). For each region the number of colours in the pie represents the number of classes for which we have high confidence in their direction of change, the +/- sign represents the direction of change and the orange, grey and yellow border represents the additional confidence derived from the multiple lines of evidence (see Box SPM.3 Table 1). {TS.4, TS Table 22}

[END BOX SPM.3, FIGURE 1 HERE]

[START FIGURE SPM.10 HERE]

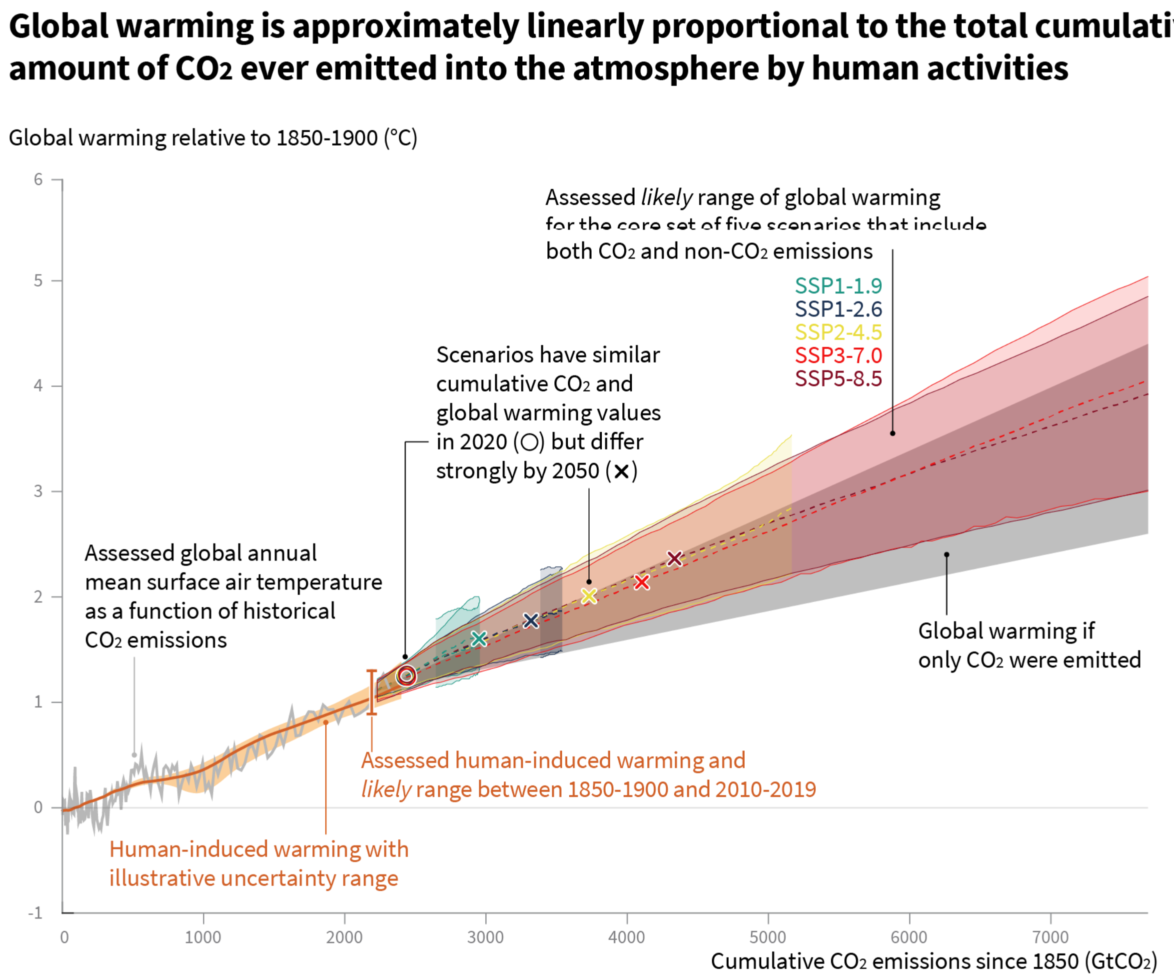

Figure SPM.10: Global mean surface air temperature increase as a function of cumulative total global CO_2 emissions. Assessed observed annual mean GSAT increase since 1850 is shown as a function of assessed historical anthropogenic CO_2 emissions (thin grey line), overlaid with an estimate of the human-induced warming (orange line) and modelled 90% uncertainty range. The grey cone shows the relationship informed by the assessed *likely* TCRE range. Coloured features show the assessed GSAT projections for the core set of five scenarios against their driving cumulative CO_2 emissions. Coloured ranges show the assessed *likely* range while dashed lines show the median. Circle and cross symbols show the location of cumulative CO_2 emissions and assessed median GSAT warming for each of the respective scenarios for the year 2020 (circles) and 2050 (crosses). {Cross-Chapter Box 2.3, 3.3, 4.3.1, 5.2, 5.5, Table 4.1, Table 5.1, Box SPM.2}

[END FIGURE SPM.10 HERE]